IEEE Access
Multidisciplinary | Rapid Review | Open Access Journal

Received September 19, 2019, accepted October 22, 2019, date of publication October 29, 2019,
date of current version November 12, 2019.

Digital Object Identifier 10.1109/ACCESS.2019.2950261

Stochastic Geometric Analysis in Cooperative Vehicular Networks Under Weibull Fading

YANG WANG[1], FUQIANG LIU[1], (Member, IEEE), CHAO WANG[1,2], (Member, IEEE), PING WANG[1], (Member, IEEE), AND YUSHENG JI[3], (Senior Member, IEEE)

[1]Department of Information and Communication Engineering, Tongji University, Shanghai 201804, China
[2]Department of Computer Science, University of Exeter, Exeter EX4 4QJ, U.K.
[3]National Institute of Informatics, Tokyo 101-8430, Japan

Corresponding author: Chao Wang (chaowang@tongji.edu.cn)

This work was supported in part by the National Natural Science Foundation of China under Grant 61771343 and Grant 61331009, in part by the European Union's Horizon 2020 Research and Innovation Programme under the Marie Sklodowska-Curie Grant 752979, in part by the Natural Science Foundation of Jiangsu Province of China under Grant BK20161165, and in part by the International Internship Program of the National Institute of Informatics, Japan.

ABSTRACT We study the performance of a cooperative vehicular communication system in a highway traffic scenario, where the locations of co-channel interfering vehicles are modeled by a one-dimensional Poisson point process (PPP). Wireless channel modeling campaigns have shown that the statistical patterns of vehicle-to-vehicle (V2V) channels can often be modeled by the Weibull distribution. Due to the complex characteristics of random fading and interference, system performance analysis is involved. To address this issue, we establish a framework for performance analysis in vehicular networks under Weibull fading and one-dimensional Poisson field of interference, where the Weibull probability density function (PDF) is approximated by a finite exponential mixture. By this means, the approximation expressions of the successful/unsuccessful message transmission probabilities for both direct V2V communication and the three-node cooperative vehicular communication are derived through stochastic geometry. Monte-Carlo simulations verify the accuracy of our derivation, as well as the advantages of encouraging cooperation among vehicles. Our methods and results can potentially be used to facilitate stochastic geometric analysis in many other complex vehicular networks under Weibull fading.

INDEX TERMS Cooperative vehicular networks, random interference, stochastic geometry, Weibull fading.

I. INTRODUCTION

As one of the key components of intelligent transportation systems (ITS), vehicular networking allows enhancing the environment awareness level of drivers, and therefore leads to great improvements in traffic safety and efficiency [1]. High-performance vehicular communications can also potentially enable individual vehicles and roadside infrastructure to share sensing, computing, and storage resources to realize the concept of vehicle cloud networks and facilitate advanced autonomous driving functions [2], [3].

Due to the rapid mobility and large number of vehicles on the road, centralized coordination of message transmissions is difficult. By contrast, distributed transmission control is often preferred. For instance, the IEEE 802.11p standard employs the carrier sense multiple access with collision avoidance (CSMA/CA) protocol for channel sharing [4]. This may lead to severe co-channel interference issues in dense scenarios [5]–[7]. The fast movement and low antenna height of vehicles also result in complicated signal propagation environments [8]. The impact of interference and fading causes reliable vehicular communications to be challenging.

Cooperative vehicular communication (CVC) is considered to be an effective solution to the above issue [9]. Allowing other vehicles in the vicinity to serve as relays provides spatial diversity [10]. Transmission coverage and reliability can both be improved. However, the performance in a cooperative communication network can be degraded by co-channel interference [11]. If the interference exhibits complicated random characteristics, the influence can be more severe and hard to quantify. Analyzing the impact of random interference on the performance in cooperative vehicular networks is of importance for directing practical system design.

Stochastic geometry is a powerful tool for random interference modeling and performance analysis, with applications in many types of wireless networks. The randomness

The associate editor coordinating the review of this manuscript and approving it for publication was Jiankang Zhang.

of interference in general comes from two major causes, i.e., the random number and location of interferers, and the random wireless fading phenomenon. Depending on application scenarios, these two factors can be mathematically modeled in different ways. For instance, vehicles driving on highway roads are typically modeled as points in the one-dimensional Cartesian coordinate system [6], [7], base stations in cellular networks can be modeled to locate in a two dimension space [12], and the random locations of unmanned aerial vehicles (UAVs) can be considered in a finite three-dimensional space [13]. The random (small-scale) fading characteristics can be modeled as Rayleigh fading [12], Nakagami-m fading [14], or certain general forms such as $\eta - \mu$ fading [15].

With such mathematical abstracts of random interference, stochastic geometry allows performance analysis in a number of wireless networks to be tractable. Examples include not only the conventional single-user point-to-point systems [12], [14], but also more sophisticated multi-antenna systems [16], multicast transmission networks [17], and cooperative communication networks [18]–[25]. The typical form of a cooperative system has a three-node network structure, with a source-destination pair and one relay terminal. The random co-channel interference is commonly modeled as *Poisson field interference*, where the locations of interfering terminals follow a Poisson point process (PPP). For a three-node decode-and-forward (DF) network, [18] quantifies the spatial-contention diversity order, which measures the relationship between system error probability and the intensity of interferers. [19] and [20] focus on the amplify-and-forward (AF) relaying protocol, and show that employing maximum ratio combining (MRC) and selection combining (SC) decoding strategies at the destination may achieve different diversity orders in the presence of random interference.

The single-relay two-hop network structure can be further extended. A K-hop DF relaying network with $K - 1$ intermediate relays is considered in [21], in which the relationship between power allocation, relay placement, and the number of hops is investigated. A closed-form expression of outage probability for such a system is derived in [22]. Multiple relays can also be activated together to assist in the transmission between the source and the destination. Reference [23] investigates the performance in a DF relaying network with MRC and SC at the destination. Reference [24] studies the potential of combining DF with AF relaying, and demonstrates the advantage of relay selection over multi-relay transmission. Reference [25] derives the performance gain of cooperative relaying with independently and randomly distributed interferers at the relays and the destination, and reveals that increasing the number of relays may not achieve extra diversity gain because of the performance bottleneck in the second hop. All these results show that in many conditions, seeking cooperation from other terminals enhances communication performance.

However, in most existing works, signal propagation between terminals is assumed to experience Rayleigh fading (e.g., [18]–[24]). This assumption permits to establish direct relationship between communication performance (normally successful transmission probability or error probability) and system parameters (such as transmission power and data rate, and intensity of interferers) due to the simple form of the channel gain distribution. But for vehicular networks, it may not be able to correctly model the actual random fading characteristics. Wireless channel modeling campaigns have shown that the vehicle-to-vehicle (V2V) channels in both urban and highway environments can often be better modeled by the Nakagami-m (or cascaded Nakagami-m [26], [27]) or Weibull fading [28]. The performance in cooperative relaying systems under Nakagami-m fading (for only integer parameter m) with randomly distributed interferers has recently been investigated in [19], [20], [25]. However, in Weibull fading environments, due to the complex density function of Weibull distribution, system performance analysis even in small and interference-free networks is very involved. Reference [29] studies the average error probability in a dual-hop AF relaying system under Weibull fading. Reference [30] analyzes the achievable effective rate over multiple-input single-output (MISO) Weibull fading channels. But these works do not take the impact of random interference into account. In vehicular communication networks with distributed transmission control, co-channel interference may play the major role in determining the bottleneck of system performance. Understanding how such interference signals, generated from randomly distributed interferers and altered by the random Weibull fading channel, influences communication quality, especially when vehicle cooperation is established, is important for system design and optimization. But to the best of our knowledge, this has not been reported in the existing literature.

In this paper, we provide such an investigation. Specifically, we consider a three-node cooperative vehicular network in a highway traffic scenario. Message delivery from the source vehicle to the destination vehicle suffers from Weibull fading and a one-dimensional Poisson field of co-channel interference. We aim to analyze system performance in terms successful decoding probability (and error probability) at the destination. To this end, we first approximate the probability density function (PDF) of Weibull distribution by a finite exponential mixture. The impact of random interference on message reception is then quantified through stochastic geometry. By this means, approximation expressions of the message recovery probabilities and error probabilities at the destination can be attained, to link communication performance with system parameters. Extensive Monte-Carlo simulations are conducted to verify the accuracy of our approximations, and also demonstrate the advantages of seeking cooperation in harsh vehicular communication systems. The main contributions of our work are summarized as follows:

- We establish a framework for performance analysis in vehicular networks under Weibull fading and one-dimensional Poisson field of interference. In particular,

we consider using a finite exponential mixture to approximate the Weibull PDF, which further enables a tractable stochastic geometric analysis on the impacts of Weibull fading and Poisson field of interference. Such a method can potentially be applied to facilitate performance evaluation and system design in many other types of wireless networks experiencing Weibull fading and random co-channel interference.

- Using the above method, we attain mathematical expressions that can accurately approximate the probabilities of successful/unsuccessful transmission for a direct V2V communication system in a highway traffic scenario. It is shown, through numerical results, that the Weibull fading phenomenon leads to very different characteristics of system performance compared with conventional Rayleigh and Nakagami-m fading. Hence analytical results reported in the existing literature are unable to provide sufficient insights.
- We derive the approximation expressions of successful/unsuccessful transmission probabilities for applying the two-phase half-duplex DF relaying protocol in a three-node cooperative vehicular network, when the destination experiences random interference and fading that remain the same or change in the two transmission phases. The relationships between system performance and different network parameters such as power, rate, channel access probability, intensity of potential interferers, are discussed in different operation regimes. The results clearly demonstrate the advantages of seeking cooperation to improve the performance in vehicular communication networks, even with complex fading and interference issues.

The remainder of the paper is organized as follows. Section II describes system model. The main idea behind approximating the Weibull PDF using a finite exponential mixture is introduced in Section III. In Section IV, we analyze the successful transmission probability and error probability for the direct source-destination transmission scheme. Section V elaborates the performance analysis for the CVC scheme in the considered cooperative vehicular network. We conclude our paper in Section VI.

Notation: Throughout the paper, we use $\mathbb{E}_X[a(X)] = \int f_X(x)a(x)\mathrm{d}x$ to denote the expectation of function $a(X)$ regarding random variable X with PDF $f_X(x)$. $\mathcal{L}_X(s) = \mathbb{E}_X[e^{-sX}]$ represents Laplace transform of non-negative random variable X. $\Gamma(x) = \int_0^\infty t^{x-1}e^{-t}\,\mathrm{d}t$ is the Gamma function. The function $(x)^+ = \max\{x, 0\}$. Let $g_1(t) = O(g_2(t))$ if $0 \leq \lim_{t\to 0}|g_1(t)/g_2(t)| < \infty$, and $g_1(t) = \Theta(g_2(t))$ if $0 < \lim_{t\to 0}|g_1(t)/g_2(t)| < \infty$ [31]. $\mathbb{R}$ denotes the set of all real values. $|\mathcal{A}|$ denotes the cardinality of set $\mathcal{A}$.

II. SYSTEM MODEL

We consider a V2V communication system in a highway traffic scenario, as shown in Fig. 1. A source vehicle S intends to transmit a message to a destination vehicle D. To enhance transmission performance in harsh vehicular communication environment, another nearby vehicle R can be activated to serve as a cooperative DF relay terminal for them, i.e., to realize CVC. The road width is assumed to be sufficiently smaller than the road length. There is no other road in the vicinity. Hence the road is modeled by an isolated straight line with infinite length, as a one-dimensional Cartesian coordinate system.[1] Without loss of generality, we consider the location and driving direction of D, when the transmission occurs, to be the origin and orientation of the coordinate system. The locations of S and R are x_s and x_r, respectively.

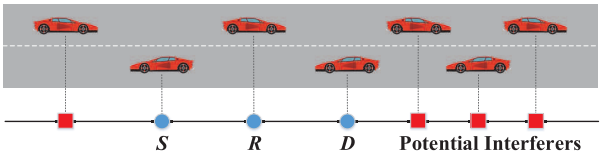

FIGURE 1. A cooperative vehicular network with Poisson field of interference.

In addition to the considered cooperative vehicular network, other vehicles driving on the highway also have demands of information exchange with their own peers. These transmitters may access the channel used by S, R, and D, and hence cause interference to them. The intensity of potential interfering vehicles is assumed to be λ vehicle/m. The slotted-Aloha MAC protocol is employed for channel sharing among these vehicles, such that at each time slot, a potential interferer is independently activated to transmit information using the channel with probability τ ($0 \leq \tau \leq 1$).

All the potential interferer vehicles locate randomly on the highway. Their positions, denoted by set $\Phi = \{x_1, x_2, \cdots\}$ with x_i being the coordinate of the ith node, are modeled by a one-dimensional homogeneous PPP, with intensity λ [6], [7]. This means, the number of potential interferers within any closed and bounded set $\mathcal{B} \subset \mathbb{R}$ is a Poisson random variable with parameter $\lambda|\mathcal{B}|$, and the numbers in disjoint sets are independent. According to the thinning property [34], thinning the parent PPP by probability τ, the locations of interferers actually transmitting in a particular time slot also follow a PPP, with intensity $\tau\lambda$ vehicle/m. The transmission in the considered cooperative vehicular network is thus affected by a *Poisson field of interference* [18].

Signal propagation between vehicles is considered to experience narrow-band Weibull block fading [35]. The channel coefficient between transmitter a and receiver b is represented by $\tilde{g}_{ab} = \sqrt{l_{ab}}g_{ab}$, where $l_{ab} = Ld_{ab}^{-\alpha}$ is path loss with constant path loss coefficient L, distance $d_{ab} = |x_a - x_b|$ and path loss exponent α, and g_{ab} is the unit-power small-scale Weibull fading coefficient. The square of a Weibull random variable is also Weibull distributed. The PDF of the channel

[1] In an urban traffic scenario, the spatial layout of roads can be modeled as a Poisson line process, and vehicles are considered to randomly locate on each road [32]. If the road is sufficiently wide with many lanes, it can be modeled as multiple parallel lines [33]. These situations are not considered in our paper.

fading power gain $h_{ab} = |g_{ab}|^2$ is

$$f_h(x;\rho,k) = \frac{k}{\rho}\left(\frac{x}{\rho}\right)^{k-1} e^{-(x/\rho)^k}, \quad x \geq 0, \tag{1}$$

where k and $\rho = \frac{1}{\Gamma(1+\frac{1}{k})}$ (since $\mathbb{E}[h_{ab}] = \rho\Gamma(1+\frac{1}{k}) = 1$) are the shape and scale parameters, respectively. The special case $k = 1$ represents the Rayleigh fading environment, since h_{ab} follows an exponential distribution. The severity of fading is indicated by the value of k. References [8] and [35] show that signal propagation in V2V channels is in general worse than that in Rayleigh fading channels, which means $k < 1$.

All vehicles transmit with power P. For CVC, the message transmission between S and D is divided into two phases due to the half-duplex operation of the relay. In the first phase, S broadcasts its message to both R and D. If R correctly recovers the source message, it repeats the message in the second phase and D performs MRC to recover the source message. If R cannot correctly decode the source signal, it remains silent in the second phase and D uses only the received signal from S in the first phase for decoding.

In phase i ($i \in \{1, 2\}$), the signal-to-interference-plus-noise ratio (SINR) between transmitter a ($a \in \{S, R\}$) and receiver b ($b \in \{R, D\}$) is

$$\mathrm{SINR}_{ab}^{[i]} = \frac{P h_{ab} l_{ab}}{\sum_{\Phi_i} P h_{v_j b} l_{v_j b} + N_0} = \frac{h_{ab} d_{ab}^{-\alpha}}{I_b^{[i]} + \eta^{-1}}, \tag{2}$$

where Φ_i denotes the set of locations of vehicles that are activated to communicate with their own peers (i.e., interferers to the receiver b in the considered network), $h_{v_j b}$ is the channel fading power gain between the jth interferer and the receiver b, $I_b^{[i]} = \sum_{\Phi_i} h_{v_j b} d_{v_j b}^{-\alpha}$ denotes *normalized* interference power, N_0 is noise power, and $\eta = PL/N_0$.

In this paper, we consider two different scenarios regarding the random characteristics of the interference terms $I_b^{[i]}$ and channel fading coefficients h_{ab}. Specifically, for the first scenario, the two transmission phases in the considered network occur in a same time slot (i.e., each phase consumes half a slot). This means, the interferers in the two phases are the same, i.e., $\Phi_1 = \Phi_2$, and all channels h_{ab} and $h_{v_j b}$ also remain unchanged. For the second scenario, however, the two transmission phases span two individual time slots. Each of the channel gains h_{ab} and $h_{v_j b}$ becomes independent in the two phases. Φ_1 is different from Φ_2, but they may have overlap because a potential interfering vehicle can be activated in both slots with probability τ^2.

At each receiver b, the source message can be successfully recovered if the effective SINR is greater than a certain value T, which is chosen according to the applied modulation and coding schemes. Therefore, in the first transmission phase, if $\mathrm{SINR}_{SR}^{[1]} > T$, R is activated to assist in the message delivery between S and D. We further assume that the power of the aggregate interference in each phase can be estimated. Then the post-MRC SINR at D is [16]

$$\mathrm{SINR}_{\mathrm{MRC}} = \mathrm{SINR}_{SD}^{[1]} + \mathrm{SINR}_{RD}^{[2]}. \tag{3}$$

As long as $\mathrm{SINR}_{\mathrm{MRC}} > T$, the source message can be successfully recovered at D. Otherwise, if R is not activated, D attains the source message only if $\mathrm{SINR}_{SD}^{[1]} > T$ in the first phase. As a result, the overall probability of successful transmission can be expressed as:

$$\mathbb{P}_{\mathrm{suc}} = \Pr\left\{\mathrm{SINR}_{SR}^{[1]} > T, \mathrm{SINR}_{\mathrm{MRC}} > T\right\} + \Pr\left\{\mathrm{SINR}_{SR}^{[1]} < T, \mathrm{SINR}_{SD}^{[1]} > T\right\}. \tag{4}$$

The probability that D is unable to recover the source message, i.e., the error probability, is thus

$$\mathbb{P}_{\mathrm{err}} = 1 - \mathbb{P}_{\mathrm{suc}}. \tag{5}$$

The derivations of $\mathbb{P}_{\mathrm{suc}}$ and $\mathbb{P}_{\mathrm{err}}$ are involved due to a number of reasons. First, the PDF of Weibull distribution is complicated. The joint impact of random interferers in Φ_i, and random fading coefficients h_{ab} as well as $h_{v_j b}$ causes finding even the expression of $\Pr\left\{\mathrm{SINR}_{ab}^{[i]} > T\right\}$ for a single V2V link to be difficult. Furthermore, in the first transmission phase, the receivers R and D are interfered by the same set of vehicles located in Φ_1. At D, the experienced interference in the two phases are also related since Φ_1 and Φ_2 may have overlap. Hence the random terms $\mathrm{SINR}_{SR}^{[1]}$, $\mathrm{SINR}_{SD}^{[1]}$, $\mathrm{SINR}_{\mathrm{MRC}}$ in (4) are dependent. The joint probability cannot be directly derived through analyzing individual events.

In the following sections, we will tackle these challenges and present approximation expressions of $\mathbb{P}_{\mathrm{suc}}$ and $\mathbb{P}_{\mathrm{err}}$.

III. APPROXIMATION OF WEIBULL PDF

Our approach to analyzing $\mathbb{P}_{\mathrm{suc}}$ and $\mathbb{P}_{\mathrm{err}}$ is based on first simplifying Weibull PDF and then applying stochastic geometry to quantify the impacts of random interference and fading. In this section, we borrow the approach proposed in [36] and explain how to approximate the Weibull PDF using a finite exponential mixture.

The moment generating function (MGF) of a Weibull random variable h is defined by substituting (1) into

$$\mathcal{M}(t) = \int_0^\infty f_h(x;\rho,k) e^{-tx}\,\mathrm{d}x.$$

Taking Taylor expansion for e^{-tx} at $t = 0$ leads to

$$\mathcal{M}(t) = \sum_{n=0}^{\infty} m_n \frac{(-t)^n}{n!} = \sum_{n=0}^{\infty} c_n t^n,$$

where $m_n = \int_0^\infty f_h(x;\rho,k) x^n\,\mathrm{d}x = \rho^n\Gamma(1+n/k)$ is the n-th order moment of h, and $c_n = (-1)^n m_n/n!$. An approximated but much simpler form of $\mathcal{M}(t)$ can be obtained by the Padé approximation (PA) technique, which uses a rational function to approximate power series. Hence we can truncate $\mathcal{M}(t)$ and apply PA as

$$\frac{\sum_{l=0}^{N} a_l t^l}{\sum_{m=0}^{M} b_m t^m} \approx \sum_{n=0}^{M+N} c_n t^n + O(t^{M+N+1}), \tag{6}$$

where both N and M are integers, with $N \leq M$. The coefficient b_0 in the rational function is set to $b_0 = 1$.

The remaining coefficients a_l and b_m can be obtained by matching the coefficients of the same powers on both sides of (6). Specifically, moving the denominator on the left hand side (LHS) to the right hand side (RHS) and ignoring all terms with order higher than t^{M+N}, one can formulate $M+N+1$ linear equations

$$\sum_{m=0}^{M} b_m c_{N-m+j} = 0, \quad 1 \le j \le M, \tag{7}$$

$$a_l = c_l + \sum_{i=1}^{\min(M,l)} b_i c_{l-i}, \quad 0 \le l \le N. \tag{8}$$

When $N = M-1$, all a_l and b_m can be obtained uniquely [37]. If the poles of the rational function are pairwise different, then the proper rational function on the LHS of (6) can be decomposed into partial fractions $\sum_{i=1}^{M} \frac{\beta_i}{t+p_i}$, for $\mathrm{Re}\{p_i\} > 0$, where p_i are the poles of the rational function and β_i are the corresponding residues. Therefore, for any $t \ge 0$, $\mathcal{M}(t)$ can be approximated as

$$\mathcal{M}(t) \approx \sum_{i=1}^{M} \frac{\beta_i}{t+p_i}. \tag{9}$$

Applying the inverse Laplace transform to both sides yields

$$f_h(x;\rho,k) \overset{(a)}{\approx} \sum_{i=1}^{M} \mathcal{L}_h^{-1}\left(\frac{\beta_i}{t+p_i}\right) \overset{(b)}{=} \sum_{i=1}^{M} \beta_i e^{-p_i x}, \tag{10}$$

where (a) follows from the linearity of inverse Laplace transform, and (b) follows from the equality $\mathcal{L}_h^{-1}(\frac{\beta_i}{t+p_i}) = \beta_i e^{-p_i x}$. Furthermore, letting $t = 0$ in (9) leads to $\sum_{i=1}^{M} \frac{\beta_i}{p_i} = 1$. In other words, the PDF of h can be expressed as the weighted sum of M exponential PDFs, because (10) can be rewritten as $f_h(x;\rho,k) \approx \sum_{i=1}^{M} \frac{\beta_i}{p_i} p_i e^{-p_i x}$. By this means, the cumulative distribution function (CDF) of the Weibull random variable h can be approximated by

$$F_h(x;\rho,k) \approx 1 - \sum_{i=1}^{M} \frac{\beta_i}{p_i} e^{-p_i x}. \tag{11}$$

The accuracy of PA is determined by the choice of M. Large M results in a better approximation result. However, the convergence becomes slower as M increases [36]. An alternative approach based on data fitting can be adopted for this issue. In general, the MGF $\mathcal{M}(t)$ of Weibull distribution does not have a closed-form expression. However, If k is a rational number[2] and can be expressed as $k = n_1/n_2$ with the minimum integers n_1 and n_2, then a simplified expression using the Meijer's G function can be obtained as [38]

$$\mathcal{M}(t) = \frac{k^{\frac{1}{2}} (\frac{n_1}{\rho t})^k}{(2\pi)^{\frac{n_1+n_2-2}{2}}} G_{n_1,n_2}^{n_2,n_1}\left(\begin{matrix}\Delta(n_1,1-k)\\ \Delta(n_2,0)\end{matrix}\middle| \frac{n_1^{n_1}}{n_2^{n_2}(\rho t)^{n_1}}\right),$$

where vector $\Delta(n,\zeta) = \left[\frac{\zeta}{n}, \frac{\zeta+1}{n}, \cdots, \frac{\zeta+n-1}{n}\right]$. Since the Meijer's G function can be computed efficiently using general numerical software such as MATLAB and Python, $\mathcal{M}(t)$ can be easily attained for any non-negative t.

Now, for some M and N, we find $\mathcal{M}(t)$ at $M+N$ properly chosen values of t, and then use a rational function $\frac{\sum_{l=0}^{N} a_l t^l}{\sum_{m=0}^{M} b_m t^m}$ to fit these realizations of MGF. It is simple to see that $a_0 = 1$, since $\mathcal{M}(0) = 1$. Hence we can obtain $M+N$ linear equations with $M+N$ unknown coefficients a_l and b_m. The unique solution exists. If we further assume that $N = M-1$, and the poles of the rational function are pairwise different, then the proper rational function (6) can be decomposed into partial fractions $\sum_{i=1}^{M} \frac{\beta_i}{t+p_i}$, for $\mathrm{Re}\{p_i\} > 0$. Therefore, again we can approximate the Weibull PDF using an exponential mixture $f_h(x;\rho,k) \approx \sum_{i=1}^{M} \beta_i e^{-p_i x}$, i.e., (10). The corresponding approximation of CDF can be expressed as the same form of (11). In fact, for relatively small M and carefully selected numerical samples of $\mathcal{M}(t)$, this method can achieve better accuracy than PA.

The approximation forms of Weibull PDF (10) and CDF (11) can facilitate tractable performance analysis in the considered cooperative vehicular network. It is shown in [39] that the exponential mixture can reach arbitrary accuracy to fit the PDF of a non-negative random variable when M goes to infinity. However, using a large value of M may cause high calculation complexity of the analytical results to be presented in the next two sections. Therefore, we consider relatively small M and adopt the second approximation method to derive the coefficients in the exponential mixture (10). Through simulations it can be seen that for the considered system with Weibull fading, finite values of M can already lead to reasonably accurate performance expressions.

IV. PERFORMANCE ANALYSIS FOR DIRECT V2V LINKS

Using the above results, we now elaborate our analysis on $\mathbb{P}_{\mathrm{suc}}$ and $\mathbb{P}_{\mathrm{err}}$ in the considered cooperative vehicular network. Our presentation starts from the performance of the direct V2V transmission between any transmitter vehicle $a \in \{S, R\}$ and receiver vehicle $b \in \{R, D\}$.

A. MATHEMATICAL ANALYSIS

We first intend to identify the probability that b can correctly recover the message of a, i.e., the SINR (2) is larger than the threshold T. Using the exact expression of Weibull CDF $F_h(x) = 1 - e^{-(x/\rho)^k}$, the probability can be written as

$$\begin{aligned}\Pr\{\mathrm{SINR}_{ab}^{[i]} > T\} &= \mathbb{E}_{I_b^{[i]}}\left[\Pr\{h_{ab} > T d_{ab}^{\alpha}(I_b^{[i]} + \eta^{-1}) | I_b^{[i]}\}\right] \\ &= \mathbb{E}_{I_b^{[i]}}\left[\exp\left(-T^k \rho^{-k} d_{ab}^{\alpha k}(I_b^{[i]} + \eta^{-1})^k\right)\right].\end{aligned}$$

When $k = 1$ (i.e., Rayleigh fading), for any non-negative value s, the expectation $\mathbb{E}_{I_b^{[i]}}[e^{-s(I_b^{[i]}+\eta^{-1})}]$ can be expressed explicitly as $e^{-s\eta^{-1}} \mathcal{L}_{I_b^{[i]}}(s) = e^{-s\eta^{-1} - \frac{2\lambda\tau s^{1/\alpha}}{\mathrm{sinc}(1/\alpha)}}$ [34], with $\mathrm{sinc}(x) = \sin(\pi x)/(\pi x)$. However, for the general Weibull fading phenomenon, i.e., $k \neq 1$, the exact form of $\mathbb{E}_{I_b^{[i]}}[e^{-s(I_b^{[i]}+\eta^{-1})^k}]$ is hard to derive and currently unknown.

[2] If k is an irrational number, then $\mathcal{M}(t)$ can be numerically approximated by its empirical Laplace transform [36].

To reach an acceptable approximation of $\Pr\{\mathrm{SINR}_{ab}^{[i]} > T\}$, we resort to the exponential mixture (10) for a certain M. Define a constant $C_{\alpha,k} = \Gamma(1-\frac{1}{\alpha})\Gamma(1+\frac{1}{\alpha k})$, for path loss exponent α and Weibull shape parameter k. The result is summarized in the following proposition.

Proposition 1: Consider V2V communication between transmitter a and receiver b, under Weibull fading and one-dimensional Poisson field of interference. With integer M, the successful transmission probability is approximated by

$$\Pr\left\{\mathrm{SINR}_{ab}^{[i]} > T\right\} \approx \sum_{j=1}^{M} \frac{\beta_j}{p_j} e^{-p_j T d_{ab}^{\alpha} \eta^{-1}} \mathcal{L}_{I_b^{[i]}}(p_j T d_{ab}^{\alpha}), \quad (12)$$

where $\mathcal{L}_{I_b^{[i]}}(s) = \mathbb{E}_{I_b^{[i]}}[e^{-sI_b^{[i]}}] = e^{-2\lambda\tau(s\rho)^{1/\alpha}C_{\alpha,k}}$ is the Laplace transform of random interference $I_b^{[i]}$, and p_i and β_i are derived in (10).

Proof: The appearance of set Φ_i and fading coefficients are independent. To separate their impacts, we first fix the set of interferers Φ_i and derive the conditional probability $\Pr\left\{\mathrm{SINR}_{ab}^{[i]} > T \middle| \Phi_i\right\}$ using (11). Afterwards, the unconditional probability $\Pr\{\mathrm{SINR}_{ab}^{[i]} > T\}$ can be found through averaging out the influence of Φ_i.

Specifically, conditioning on any particular Φ_i, we have

$$\begin{aligned}
&\Pr\left\{\mathrm{SINR}_{ab}^{[i]} > T \middle| \Phi_i\right\} \\
&= \Pr\left\{h_{ab} > T d_{ab}^{\alpha}(I_b^{[i]} + \eta^{-1}) \middle| \Phi_i\right\} \\
&\overset{(a)}{=} \mathbb{E}_{\mathbf{h}_b^{[i]}}\left[\int_{T d_{ab}^{\alpha}(I+\eta^{-1})}^{\infty} f_{h_{ab}}(x;\rho,k)\,\mathrm{d}x \middle| \Phi_i\right] \\
&\overset{(b)}{\approx} \sum_{j=1}^{M} \frac{\beta_j}{p_j} \mathbb{E}_{\boldsymbol{h}_b^{[i]}}\left[e^{-p_j T d_{ab}^{\alpha}(I_b^{[i]}+\eta^{-1})} \middle| \Phi_i\right], \quad (13)
\end{aligned}$$

where $\boldsymbol{h}_b^{[i]} = [h_{v_1 b}, h_{v_2 b}, \cdots]$ is the small-scale interference (generated by interferers within Φ_i) channel vector, the expectation in step (a) is taken over $\boldsymbol{h}_b^{[i]}$, and (b) follows from (11). Therefore, the unconditional probability

$$\begin{aligned}
\Pr\left\{\mathrm{SINR}_{ab}^{[i]} > T\right\} &= \mathbb{E}_{\Phi_i}\left[\Pr\left\{\mathrm{SINR}_{ab}^{[i]} > T \middle| \Phi_i\right\}\right] \\
&\approx \sum_{j=1}^{M} \frac{\beta_j}{p_j} \exp(-p_j T \eta^{-1} d_{ab}^{\alpha}) \mathcal{L}_{I_b^{[i]}}(p_j T d_{ab}^{\alpha}). \quad (14)
\end{aligned}$$

The Laplace transform of interference, i.e., $\mathcal{L}_{I_b^{[i]}}(s)$, can be obtained by borrowing the result given in [34, pp. 103] as

$$\begin{aligned}
\mathcal{L}_{I_b^{[i]}}(s) &\overset{(a)}{=} \mathbb{E}_{\Phi_i}\left[\prod_{v_j \in \Phi_i} \mathbb{E}_h\left[e^{-shd_{v_j b}^{-\alpha}}\right]\right] \\
&\overset{(b)}{=} \exp\Big(-\lambda\tau \int_{\mathbb{R}} \left(1 - \mathbb{E}_h[e^{-sh|x|^{-\alpha}}]\right) \mathrm{d}x\Big) \\
&= \exp\Big(-2\lambda\tau s^{1/\alpha} \mathbb{E}_h[h^{1/\alpha}]\Gamma(1-1/\alpha)\Big), \quad (15)
\end{aligned}$$

where (a) follows from the fact that the small-scale fading gains of different links are independent, (b) follows from the probability generating functional (PGFL) of PPP (i.e., $\mathbb{E}_{\Psi}[\prod_{x_i \in \Psi} f(x_i)] = e^{-\lambda_0 \int_{\mathbb{R}} (1-f(x))\,\mathrm{d}x}$ for one-dimensional PPP Ψ with intensity λ_0 and any function $f(x)$ such that $0 \le f(x) \le 1$ and $1-f(x)$ is integrable on $\mathbb{R}$), and h is a Weibull distributed random variable with the same parameters as h_{ab}. The fractional moment of h is

$$\mathbb{E}[h^{1/\alpha}] = \int_0^{\infty} x^{1/\alpha} f_h(x;\rho,k)\,\mathrm{d}x = \rho^{1/\alpha}\Gamma(1+\frac{1}{\alpha k}). \quad (16)$$

Substituting (15) and (16) into (14) proves the proposition. ■

Proposition 1 provides a closed-form expression of the approximated successful transmission probability for a V2V link when signal propagation experiences Weibull fading. The accuracy of the approximation depends on the choice of the parameter M. Larger M leads to better approximation, but potentially higher calculation complexity when we derive the performance of the CVC scheme in the next section.

In addition to enabling system performance analysis in the considered cooperative vehicular network, setting a to be S and b to be D yields the successful transmission probability for the direct transmission (DT) between S and D without relaying. Equation (12) establishes an explicit relationship between performance (successful/unsuccessful transmission probabilities) and system parameters (transmission power, data rate, activation probability, etc.). Hence it can be used for facilitating more complex performance analysis such as quantifying the average number of vehicles that can correctly receive a transmitting vehicle's broadcast heartbeat messages [40]. System design including power and rate control can also be potentially conducted.

If $\tau\lambda = 0$ (i.e., the intensity of interferers is zero), the set of interferers Φ_i is an empty set. In such an interference-free environment, it is straightforward to attain, from the CDF of Weibull distribution, that $\Pr\{\mathrm{SINR}_{ab}^{[i]} < T\} \propto \left(\frac{P}{N_0}\right)^{-k}$ for sufficiently large signal-to-noise ratio (SNR) $\frac{P}{N_0}$. The achievable diversity gain is k, which is smaller than 1, the diversity gain for the Rayleigh fading environment, when $k < 1$. In this case, signal propagation in V2V channels experiences severer fading phenomenon than Rayleigh fading.

Furthermore, in the case $k < 1$, if $\tau\lambda \to 0$ and $\frac{P}{N_0} \to \infty$, then by taking Taylor expansion $e^{-x} \to 1 - x$ in (12) and letting $M \to \infty$ to achieve equivalence, we can see that $\Pr\{\mathrm{SINR}_{ab}^{[i]} < T\} = \Theta(\tau\lambda)$, i.e., the spatial-contention diversity order [18] $\lim_{\tau\lambda\to 0} \frac{\log \Pr\{\mathrm{SINR}_{ab}^{[i]} < T\}}{\log(\tau\lambda)} = 1$. If a proper scheduling strategy is conducted to manage the transmissions of vehicles driving on the highway road such that the intensity of random interferers is sufficiently small, the high-SNR error probability of a direct V2V communication link would scale with the intensity $\tau\lambda$.

B. NUMERICAL RESULTS

The accuracy of our approximation approach can be validated through simulations. To this end, we consider DT between S and D, using the capacity-achieving Gaussian random code with rate r bit/codeword. (In this case, the error probability

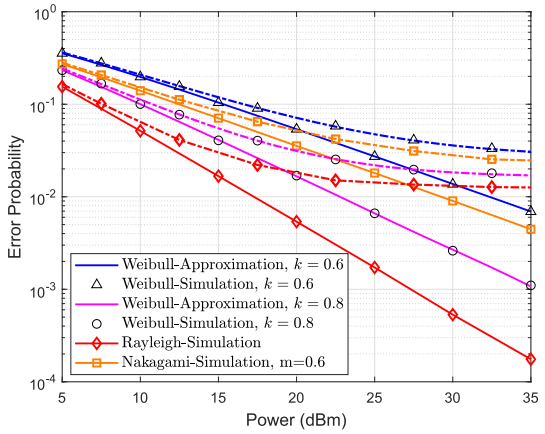

FIGURE 2. Error probability of DT in different fading environments, with $r = 1$ bit/codeword, and $\lambda = 0.01$ vehicle/m. Solid lines and dash lines represent $\tau = 0$ (i.e. interference-free) and $\tau = 4 \times 10^{-3}$, respectively.

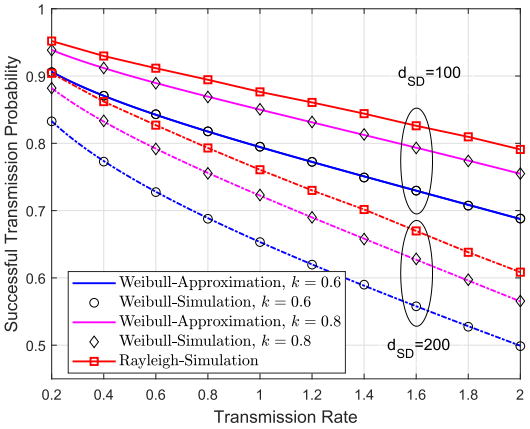

FIGURE 3. Successful transmission probability of DT with $\lambda = 0.1$ vehicle/m, $\tau = 4 \times 10^{-3}$, and $P = 20$ dBm.

equals channel outage probability.) The transmission process consumes one time slot, so that the SINR threshold $T = 2^r - 1$. The noise power is set to be $N_0 = -99$ dBm. The distance between S and D is $|x_s| = 100$ m. The path loss exponent $\alpha = 2$ and path loss coefficient $L = 650^{-2}$ [41]. In Fig. 2, we plot the error probability $\Pr\left\{\text{SINR}_{ab}^{[i]} < T\right\}$ versus transmission power P, for two different Weibull fading characteristics. Specifically, we set $k = 0.8$ and $k = 0.6$, for which $M = 4$ and $M = 6$ are used respectively in the approximations. For comparison, we also illustrate the performance in Rayleigh and Nakagami-m fading environments.

From the figure, it can be seen that the error probability approximation expression presented in Proposition 1 is closely in line with simulation results, even with finite values of M. From the interference-free condition, i.e., when $\tau\lambda = 0$, we can observe that the V2V transmission under Weibull fading has lower achievable diversity gain than that under Rayleigh fading. Even though we can properly choose the parameter m for Nakagami-m fading so that transmission in both cases achieve the same diversity gain (for the case $k = 0.6$) in the interference-free environment, when complicated interference generated by random interferers is taken into consideration, the error performances in different fading environments exhibit very different patterns. Thus the stochastic geometric analysis in existing works cannot be directly applied when signal propagation in V2V channels experiences Weibull fading. A smaller value of k leads to worse performance and when P increases, the error probability starts to reach an error floor because of interference.

In Fig. 3, we plot the relationship between the probability of successful transmission and transmission data rate r. Again, the approximation presented in Proposition 1 well matches the simulation results. The simple closed-form approximation expression establishes the relationship between communication performance and system parameters, and thus can be potentially used for both performance analysis and further system design such as rate adaptation or power allocation. In general, message delivery in Weibull fading channels with $k < 1$ has worse performance than that in a Rayleigh fading environment. For the same system setup, a smaller value of k leads to a lower probability of successful transmission. Having a larger distance between the source and destination also degrades system performance. Seeking cooperation from nearby vehicles can be an effective solution to this issue, which will be shown in the following section.

V. PERFORMANCE ANALYSIS FOR CVC

Now we present the approximation expressions of the successful transmission probability (4) (and also the error probability (5)) for the CVC scheme. As mentioned in Section II, in the first phase, the receptions of R and D are affected by the same set of interfering vehicles in Φ_1. This causes $\text{SINR}_{SR}^{[1]}$, $\text{SINR}_{SD}^{[1]}$, and SINR_{MRC} to be correlated. The interferer sets Φ_1 and Φ_2 may have possible overlap. One cannot directly attain $\mathbb{P}_{\text{suc}}$ by individually deriving $\Pr\{\text{SINR}_{SR}^{[1]} > T\}$, $\Pr\{\text{SINR}_{SD}^{[1]} > T\}$ and $\Pr\{\text{SINR}_{\text{MRC}} > T\}$.

Two different cases regarding the random interference and fading are investigated. The first case refers to that the two transmission phases of CVC occur in the same time slot, so that $\Phi_1 = \Phi_2$ and all small-scale fading coefficients remain unchanged. In the second scenario, each transmission phase consumes one time slot. Interferers may not be identical and the fading coefficients change independently and randomly. In what follows, we first elaborate mathematical analysis on (4), and then provide simulation results and discussions.

A. MATHEMATICAL ANALYSIS

To facilitate presentation, let us define a number of functions as follows. First, with the distance between R and D, $d_{RD} = |x_r|$, and path loss component α, a function of non-negative arguments $\sigma_1 \geq 0$ and $\sigma_2 \geq 0$ is defined as

$$\mathcal{I}_0(\sigma_1, \sigma_2) = \int_{\mathbb{R}} \left(1 + \sigma_1 |x|^\alpha\right)^{-1} \left(1 + \sigma_2 |x - d_{RD}|^\alpha\right)^{-1} \mathrm{d}x. \tag{17}$$

For any σ_1 and σ_2, the integration can be easily attained by numerical methods. When $\alpha = 2$, by using the residues theorem [42], a closed-form expression can be obtained as

$$\mathcal{I}_0(\sigma_1, \sigma_2) = \frac{\pi\left(\sigma_1^{1/2} + \sigma_2^{1/2}\right)}{\sigma_1\sigma_2 d_{RD}^2 + \left(\sigma_1^{1/2} + \sigma_2^{1/2}\right)^2}. \tag{18}$$

In addition, for any $\sigma > 0$, we have

$$\mathcal{I}_0(\sigma, 0) = \mathcal{I}_0(0, \sigma) = \frac{2\sigma^{-1/\alpha}}{\mathrm{sinc}(1/\alpha)}. \tag{19}$$

Based on $\mathcal{I}_0(\sigma_1, \sigma_2)$, and using the Weibull fading coefficients k and ρ, the PDF approximation coefficients M, p_i, β_i for $i \in \{1, 2, \cdots, M\}$ in (10), and constant $C_{\alpha,k} = \Gamma(1 - \frac{1}{\alpha})\Gamma(1 + \frac{1}{\alpha k})$, three other functions are defined as

$$\begin{aligned}
&\mathcal{I}_1(\sigma_1', \sigma_2') \\
&= 2\left((\rho\sigma_1')^{1/\alpha} + (\rho\sigma_2')^{1/\alpha}\right)C_{\alpha,k} \\
&\quad - \sum_{i=1}^{M}\sum_{j=1}^{M} \frac{\beta_i\beta_j}{p_ip_j}\mathcal{I}_0\left(\frac{p_i}{\sigma_1'}, \frac{p_j}{\sigma_2'}\right),
\end{aligned} \tag{20}$$

$$\begin{aligned}
&\mathcal{I}_2(s_1, s_2, s_3) \\
&= \frac{s_1\left(\mathcal{I}_0(s_1^{-1}, 0) - \mathcal{I}_0(s_1^{-1}, s_3^{-1})\right)}{s_1 - s_2} \\
&\quad - \frac{s_2\left(\mathcal{I}_0(s_2^{-1}, 0) - \mathcal{I}_0(s_2^{-1}, s_3^{-1})\right)}{s_1 - s_2} + \mathcal{I}_0(0, s_3^{-1}),
\end{aligned} \tag{21}$$

$$\begin{aligned}
&\mathcal{I}_3(s_1', s_2', s_3') \\
&= \tau(1-\tau)\left(\mathcal{I}_1(s_1', s_3') + 2(\rho s_2')^{\frac{1}{\alpha}}C_{\alpha,k}\right) \\
&\quad + \tau^2\sum_{l=1}^{M}\sum_{i=1}^{M}\sum_{j=1}^{M}\frac{\beta_l\beta_i\beta_j}{p_lp_ip_j}\mathcal{I}_2\left(\frac{s_1'}{p_i}, \frac{s_2'}{p_j}, \frac{s_3'}{p_l}\right).
\end{aligned} \tag{22}$$

In general, these three functions can be evaluated straightforwardly using numerical methods. For the special case $\alpha = 2$, closed-form expressions are attainable based on (18). Now, we present our results, starting from the first scenario.

1) CVC OCCURRING IN ONE TIME SLOT

Since both interferers and fading coefficients are the same in the two transmission phases, $I_D^{[1]}$ and $I_D^{[2]}$ are identical. In this case, the effective SINR at D after MRC is

$$\mathrm{SINR}_{\mathrm{MRC}} = \frac{h_{SD}d_{SD}^{-\alpha} + h_{RD}d_{RD}^{-\alpha}}{I_D^{[1]} + \eta^{-1}}, \tag{23}$$

where $I_D^{[1]} = \sum_{\Phi_1} h_{v_jD}d_{v_jD}^{-\alpha}$ is the normalized interference experienced by D in both phases. The expression of an approximation of the overall decoding probability at the destination is given in the following proposition.

Proposition 2: Consider a three-node half-duplex cooperative vehicular network, under Weibull fading and one-dimensional Poisson field of interference. When the two transmission phases occur in the same time slot, with integer M, the probability of successful transmission can be approximated by (24), as shown at the bottom of this page, where $\mathcal{L}_{I_D^{[i]}}(s) = e^{-2\lambda\tau(s\rho)^{1/\alpha}C_{\alpha,k}}$, $\psi_1 = d_{SD}^{\alpha}(T - z)^+$, $\psi_2 = zd_{RD}^{\alpha}$, and $\psi_3 = Td_{SR}^{\alpha}$.

Proof: Here we provide only a brief explanation of the intuition of the proof. Details are elaborated in Appendix A.

Since $\Pr\{\mathrm{SINR}_{SR}^{[1]} < T, \mathrm{SINR}_{SD}^{[1]} > T\} = \Pr\{\mathrm{SINR}_{SD}^{[1]} > T\} - \Pr\{\mathrm{SINR}_{SR}^{[1]} > T, \mathrm{SINR}_{SD}^{[1]} > T\}$, we can further express $\mathbb{P}_{\mathrm{suc}}$ in (4) as $\mathbb{P}_{\mathrm{suc}} = \Pr\{\mathrm{SINR}_{SD}^{[1]} > T\} - \Pr\{\mathrm{SINR}_{SR}^{[1]} > T, \mathrm{SINR}_{SD}^{[1]} > T\} + \Pr\{\mathrm{SINR}_{SR}^{[1]} > T, \mathrm{SINR}_{\mathrm{MRC}} > T\}$. We can individually derive these three probabilities to reach $\mathbb{P}_{\mathrm{suc}}$. From Proposition 1, we know $\Pr\{\mathrm{SINR}_{SD}^{[1]} > T\} = \sum_{j=1}^{M}\frac{\beta_j}{p_j}e^{-p_jTd_{SD}^{\alpha}\eta^{-1}}\mathcal{L}_{I_D^{[i]}}(p_jTd_{SD}^{\alpha})$. The key is then to derive the remaining two probabilities.

Start from $\Pr\{\mathrm{SINR}_{SR}^{[1]} > T, \mathrm{SINR}_{SD}^{[1]} > T\}$. Because the occurrence of set Φ_1 and all fading coefficients are independent, for a fixed set of interferers Φ_1, the events $\mathrm{SINR}_{SR}^{[1]} > T$ and $\mathrm{SINR}_{SD}^{[1]} > T$ are independent. This means $\Pr\{\mathrm{SINR}_{SR}^{[1]} > T, \mathrm{SINR}_{SD}^{[1]} > T\big|\Phi_1\} = \Pr\{\mathrm{SINR}_{SR}^{[1]} > T\big|\Phi_1\}\Pr\{\mathrm{SINR}_{SD}^{[1]} > T\big|\Phi_1\}$. By using (13), $\Pr\{\mathrm{SINR}_{SR}^{[1]} > T\big|\Phi_1\}$ can be approximated as $\sum_{j=1}^{M}\frac{\beta_j}{p_j}\mathbb{E}_{\boldsymbol{h}_R^{[1]}}\left[e^{-p_jTd_{SR}^{\alpha}(I_R^{[i]}+\eta^{-1})}\big|\Phi_1\right]$, and similarly $\Pr\{\mathrm{SINR}_{SD}^{[1]} > T\big|\Phi_1\}$ can be approximated as $\sum_{j=1}^{M}\frac{\beta_j}{p_j}\mathbb{E}_{\boldsymbol{h}_D^{[1]}}\left[e^{-p_jTd_{SR}^{\alpha}(I_D^{[i]}+\eta^{-1})}\big|\Phi_1\right]$. Consequently, the original joint probability can be attained by taking the expectation of the conditional probability regarding Φ_1, i.e., $\sum_{l=1}^{M}\sum_{j=1}^{M}\frac{\beta_l\beta_j}{p_lp_j}e^{-\frac{p_lw_1+p_jw_2}{\eta}}\mathbb{E}_{\Phi_i}[e^{-w_1I_D^{[i]}-w_2I_R^{[i]}}]$, with $w_1 = Td_{SD}^{\alpha}$ and $w_2 = Td_{SR}^{\alpha}$. The result can be obtained by using the PGFL of PPP [34] and (10), which is the second term in (24).

Similarly, for the term $\Pr\{\mathrm{SINR}_{SR}^{[1]} > T, \mathrm{SINR}_{\mathrm{MRC}} > T\}$, the two events $\mathrm{SINR}_{SR}^{[1]} > T$ and $\mathrm{SINR}_{\mathrm{MRC}} > T$ are conditionally independent given Φ_1 (recall that $\Phi_1 = \Phi_2$). The conditional probability $\Pr\{\mathrm{SINR}_{SR}^{[1]} > T|\Phi_1\}$ can be found following the proof of Proposition 1. Regarding the conditional probability $\Pr\{\mathrm{SINR}_{\mathrm{MRC}} > T|\Phi_1\}$, using (10) we can attain this probability to be $-\sum_{i=1}^{M}\sum_{j=1}^{M}\frac{\beta_i\beta_j}{p_ip_j}\int_{\mathbb{R}}\frac{\mathrm{d}}{z\mathrm{d}s} \times \left[e^{-\frac{p_i\psi_1+sp_j\psi_2}{\eta}}\prod_{x_i\in\Phi_1}\mathbb{E}_h\left[e^{-\frac{(p_i\psi_1+sp_j\psi_2)h}{|x_i|^{\alpha}}}\right]\right]\Big|_{s=1}\mathrm{d}z$, where h is a

$$\begin{aligned}
\mathbb{P}_{\mathrm{suc}} \approx &\sum_{j=1}^{M}\frac{\beta_j}{p_j}e^{-p_jTd_{SD}^{\alpha}\eta^{-1}}\mathcal{L}_{I_D^{[i]}}(p_jTd_{SD}^{\alpha}) - \sum_{i=1}^{M}\sum_{j=1}^{M}\frac{\beta_i\beta_j}{p_ip_j}\exp\Big(-\frac{p_iTd_{SR}^{\alpha} + p_jTd_{SD}^{\alpha}}{\eta} - \lambda\tau\mathcal{I}_1(p_iTd_{SR}^{\alpha}, p_jTd_{SD}^{\alpha})\Big) \\
&- \sum_{l=1}^{M}\sum_{i=1}^{M}\sum_{j=1}^{M}\frac{\beta_l\beta_i\beta_j}{p_lp_ip_j}\int_0^{\infty}\frac{\mathrm{d}}{z\mathrm{d}s}\exp\Big(-\frac{p_i\psi_1 + sp_j\psi_2 + p_l\psi_3}{\eta} - \lambda\tau\mathcal{I}_1(p_i\psi_1 + sp_j\psi_2, p_l\psi_3)\Big)\Big|_{s=1}\mathrm{d}z
\end{aligned} \tag{24}$$

Weibull random variable with parameters k and ρ. Again, the joint probability $\Pr\{\mathrm{SINR}_{SR}^{[1]} > T, \mathrm{SINR}_{\mathrm{MRC}} > T\}$ can be found by taking the expectation regarding Φ_1, using the PGFL of PPP. This is the last term in (24). ■

Although equation (24) contains integrals that in general do not have simple closed-form expressions, these integrals can be easily calculated using numerical methods, e.g., the Gauss-Chebyshev quadrature, through common mathematical software such as MATLAB and Python. As we mentioned earlier, if $\alpha = 2$, a closed-form expression of $\mathcal{I}_0(s_1, s_2)$ given in (17) can be explicitly found as (18). Then the expression of $\mathbb{P}_{\mathrm{suc}}$ can be further simplified, which only contains a number of definite integrals. Hence the relationship between system performance and parameters, with Weibull fading and random interferers, is also established mathematically. In an interference-free environment, i.e., when $\tau\lambda = 0$, for $P \to \infty$ we can obtain that $\Pr\{\mathrm{SINR}_{\mathrm{MRC}} < T\} \propto (\frac{P}{N_0})^{-2k}$ from [43, eq. (30)]. Together with the fact that $\Pr\{\mathrm{SINR}_{ab}^{[i]} < T\} \propto (\frac{P}{N_0})^{-k}$, we can prove that $\mathbb{P}_{\mathrm{err}} \propto (\frac{P}{N_0})^{-2k}$. Therefore, the achievable diversity gain doubles that of DT. Encouraging cooperation among vehicles is clearly advantageous.

As shown in Fig. 2, in the high SNR regime the random interference causes error floor, which would also occur in the CVC scheme. A proper transmission scheduling strategy should be able to manage the interference level experienced by each vehicle so that high-quality message delivery can be realized. In the considered system, the interference can be limited by adapting the activation rate τ according to the intensity λ of vehicles on the road. Following Proposition 2, we can further attain a relationship between high-SNR error probability $\mathbb{P}_{\mathrm{err}}$ (i.e., the error floor) and the intensity of interfering vehicles, i.e., $\tau\lambda$. The result is summarized in the following corollary.

Corollary 1: In the considered cooperative vehicular network under Weibull fading with $k < 1$ and one-dimensional Poisson field of interference, when the CVC consumes one time slot, the system's decoding error probability scales linearly with $\tau\lambda$, i.e., $\mathbb{P}_{\mathrm{err}} = \Theta(\tau\lambda)$, for $\tau\lambda \to 0$ and $P \to \infty$.

Proof: The proof can be found in Appendix B. ■

This result means that the spatial-contention diversity order $\lim_{\lambda\tau\to 0} \frac{\log \mathbb{P}_{\mathrm{err}}}{\log(\lambda\tau)} = 1$, same as the case in DT. It helps understand the impact of potential interference management solutions on system performance in the high-SNR weak-interference regime. Its accuracy will be shown through simulations in Section V-B.

2) CVC OCCURRING IN TWO TIME SLOTS

Now we focus on the case that the two interferer sets Φ_1 and Φ_2 are not identical, and all channel fading coefficients change independently in the two CVC phases. This situation can happen if the source's broadcasting and relay's forwarding phases are separated by a sufficiently large interval (compared to the coherence time of the wireless channel) and thus span two individual time slots. Note that Φ_1 and Φ_2 may still have overlap because every vehicle on the road has probability τ^2 to be activated in both slots. The effective SINR at D after MRC is now

$$\mathrm{SINR}_{\mathrm{MRC}} = \frac{h_{SD} d_{SD}^{-\alpha}}{I_D^{[1]} + \eta^{-1}} + \frac{h_{RD} d_{RD}^{-\alpha}}{I_D^{[2]} + \eta^{-1}}. \tag{25}$$

The expression of $\mathbb{P}_{\mathrm{suc}}$ is different from that presented in Proposition 2, and is provided as follows.

Proposition 3: Consider a three-node half-duplex cooperative vehicular network, under Weibull fading and one-dimensional Poisson field of interference. When the two transmission phases occur in two different time slots, with integer M, the probability of successful transmission can be approximated by (26), where $\mathcal{L}_{I_D^{[i]}}(s) = e^{-2\lambda\tau(s\rho)^{1/\alpha} C_{\alpha,k}}$, $\psi_1 = d_{SD}^{\alpha}(T-z)^{+}$, $\psi_2 = z d_{RD}^{\alpha}$, and $\psi_3 = T d_{SR}^{\alpha}$.

Proof: The basic proof process is similar to that for Proposition 2. The probability $\mathbb{P}_{\mathrm{suc}}$ in (4) can be expressed as the sum of three probabilities: $\mathbb{P}_{\mathrm{suc}} = \Pr\{\mathrm{SINR}_{SD}^{[1]} > T\} - \Pr\{\mathrm{SINR}_{SR}^{[1]} > T, \mathrm{SINR}_{SD}^{[1]} > T\} + \Pr\{\mathrm{SINR}_{SR}^{[1]} > T, \mathrm{SINR}_{\mathrm{MRC}} > T\}$. Approximations of the first two can be found by following the proof of Proposition 2.

Regarding the term $\Pr\{\mathrm{SINR}_{SR}^{[1]} > T, \mathrm{SINR}_{\mathrm{MRC}} > T\}$, the two events $\mathrm{SINR}_{SR}^{[1]} > T$ and $\mathrm{SINR}_{\mathrm{MRC}} > T$ are conditionally independent given Φ_1 and Φ_2. By identifying the approximations of the conditional probabilities $\Pr\{\mathrm{SINR}_{SR}^{[1]} > T|\Phi_1\}$ and $\Pr\{\mathrm{SINR}_{\mathrm{MRC}} > T|\Phi_1, \Phi_2\}$, the original unconditional joint probability can be obtained by taking the expectation of their product, with respect to both Φ_1 and Φ_2, using the PGFL of PPP. All the results are summarized by (26). The detailed proof is presented in Appendix C. ■

Similar to the case presented in Proposition 2, for given system parameters, the approximated successful transmission probability (26), as shown below, can be evaluated by numerical methods. When $\alpha = 2$, a closed-form of $\mathcal{I}_0(s_1, s_2)$ can be found as (18). Thus the overall successful transmission probability $\mathbb{P}_{\mathrm{suc}}$ can be computed more efficiently. For the

$$\mathbb{P}_{\mathrm{suc}} \approx \sum_{j=1}^{M} \frac{\beta_j}{p_j} e^{-p_j T d_{SD}^{\alpha} \eta^{-1}} \mathcal{L}_{I_D^{[i]}}(p_j T d_{SD}^{\alpha}) - \sum_{i=1}^{M}\sum_{j=1}^{M} \frac{\beta_i \beta_j}{p_i p_j} \exp\Big(- \frac{p_i T d_{SR}^{\alpha} + p_j T d_{SD}^{\alpha}}{\eta} - \lambda\tau \mathcal{I}_1(p_i T d_{SR}^{\alpha}, p_j T d_{SD}^{\alpha})\Big)$$
$$- \sum_{l=1}^{M}\sum_{i=1}^{M}\sum_{j=1}^{M} \frac{\beta_l \beta_i \beta_j}{p_l p_i p_j} \int_0^{\infty} \frac{\mathrm{d}}{z\mathrm{d}s} \exp\Big(- \frac{p_i \psi_1 + s p_j \psi_2 + p_l \psi_3}{\eta} - \lambda\tau \mathcal{I}_3(p_i\psi_1, s p_j \psi_2, p_l \psi_3)\Big)\Big|_{s=1} \mathrm{d}z \tag{26}$$

interference-free environment $\tau\lambda = 0$, since the error probability is the same as that in the previous scenario, the diversity gain is also $2k$.

In addition, the relationship between high-SNR error probability $\mathbb{P}_{\text{err}}$ and the intensity of interfering vehicles on the road $\tau\lambda$ can also quantified for the weak-interference scenario. The following corollary presents the result.

Corollary 2: In the considered cooperative vehicular network under Weibull fading with $k < 1$ and one-dimensional Poisson field of interference, when the CVC consumes two separate time slots, $\tau\lambda \to 0$ and $P \to \infty$, the decoding error probability scales linearly with $\tau\lambda$, i.e., $\mathbb{P}_{\text{err}} = \Theta(\tau\lambda)$, except for the case $d_{SR} \to 0$ in which $\mathbb{P}_{\text{err}}$ scales linearly with $\lambda\tau^2$ as $\mathbb{P}_{\text{err}} = \Theta(\lambda\tau^2)$.

Proof: The proof is provided in Appendix D. ■

This result is not the same as that in Corollary 1, in which the high-SNR error probability is proportional to $\tau\lambda$ irrespective of the position of the relay. By contrast, when the interferer set and fading coefficients change independently in the two transmission phases, the error probability would scale with $\lambda\tau^2$ if the relay is extremely close to the source. This means that requiring S itself to retransmit its message in the second phase would lead to better performance than seeking cooperation. However, this is valid for only the high SNR regime, where the impact of large-scale fading is limited. If $\tau\lambda$ is reasonably large and P is finite, relaying through vehicular cooperation is still advantageous. System design can be guided by the result shown in Proposition 3.

B. NUMERICAL RESULTS

Now we validate the effectiveness of our analytical results given in the above two subsections through simulations. The simulation parameters are chosen to be the same as those in Section IV: $\alpha = 2$, $N_0 = -99$ dBm, $L = 650^{-2}$ [41]. We set $k = 0.6$, and the corresponding value of M in (10) as $M = 6$. For fair comparisons with DT, we require the transmission rate of S and R to be $2r$ bit/codeword, so that the threshold $T = 2^{2r-1}$. By this means, the average transmission rate remains to be r bit/slot, same as that of DT.

Fig. 4 displays the error probability comparison, when the transmission power of different vehicles changes. The distance between S and D is set to be $d_{SD} = 200$ m, and R is assumed to locate in the middle, i.e., $d_{SR} = d_{RD} = 100$ m. From the figure we can see that our approximation expressions well match simulation results, which verifies the accuracy of the results shown in Propositions 2 and 3. In the interference-free environment, vehicular cooperation (the two scenarios have the same error probability, and thus only one curve is plotted) leads to higher diversity gain compared with DT. When the receptions suffer from random co-channel interference, cooperation also provides smaller error probability. Hence seeking assistance from nearby vehicles can improve the performance of vehicular communications even in environments with complex fading and interference issues. For high SNR, inevitably error floor occurs due to strong interference. In addition, we display the

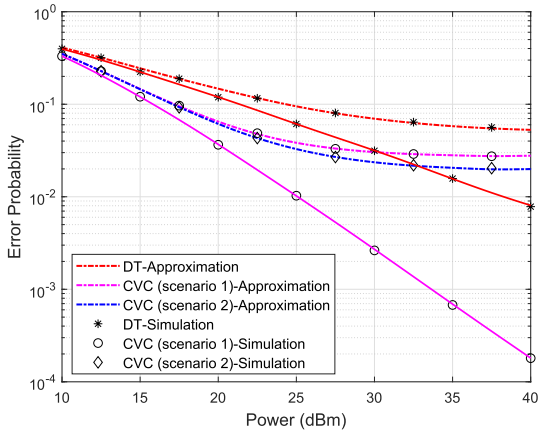

FIGURE 4. Error probability of CVC, with $\lambda = 0.01$ vehicle/m, and $r = 1$ bit/codeword. Solid lines and dashed lines represent $\tau = 0$ (i.e., interference-free environment), and $\tau = 4 \times 10^{-3}$, respectively.

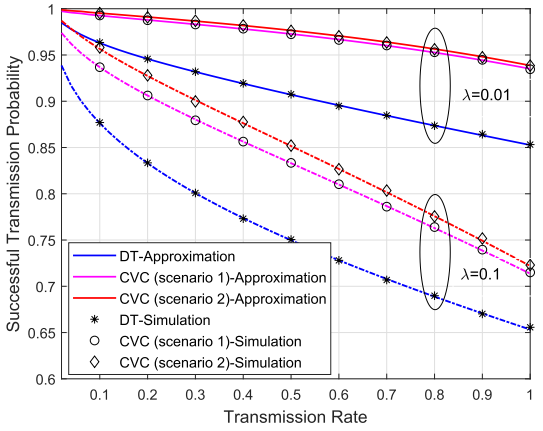

FIGURE 5. Successful transmission probability of CVC with $\tau = 4 \times 10^{-3}$, and $P = 20$ dBm.

impact of the transmission rate r on the successful transmission probability $\mathbb{P}_{\text{suc}}$ in Fig. 5. Again, our approximation expressions are closely in line with simulation results. Cooperation leads to higher transmission reliability than DT. As expected, higher vehicle density λ leads to smaller achievable $\mathbb{P}_{\text{suc}}$, because of increased interference. In these situations, proper user scheduling and resource allocation (e.g., power and rate control, relay selection) strategies should be conducted to improve performance. Such system design and optimization can potentially be guided by our analytical results.

Finally, we consider the high-SNR weak-interference scenario, i.e., when $\tau\lambda \to 0$, and verify the results shown in Corollary 1 and Corollary 2. We set $d_{SD} = 100$ m, and display the relationship between error probability $\mathbb{P}_{\text{err}}$ and channel access probability τ, for a sufficiently large power level P and different positions of relay (controlled by the ratio $\frac{d_{SR}}{d_{SD}}$), in Fig. 6. Clearly, for scenario 1, in which both the set of interferers and channel fading environments remain unchanged in the whole transmission process, $\log \mathbb{P}_{\text{err}}$ always scales linearly with $\log \tau$ (since λ is fixed). The slopes are

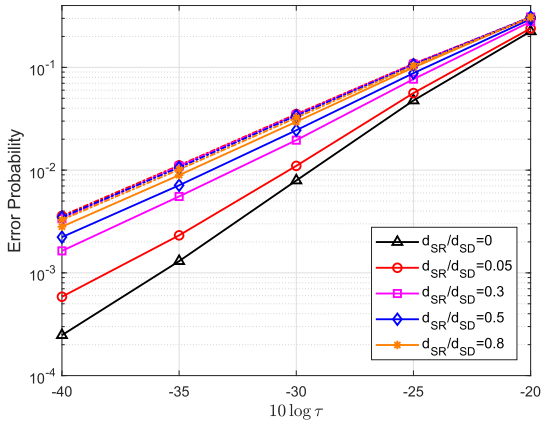

FIGURE 6. Error probability of CVC in high-SNR weak-interference environment, with $r = 1$ bit/codeword, $P = 40$ dBm, $\lambda = 0.1$ vehicle/m. Dashed lines and solid lines represent scenario 1 and scenario 2, respectively.

not affected by the position of the relay. On the other hand, for the second scenario, in which interfering vehicles and channel gains both change in the two transmission phases, having a relay very close to the source would lead to a larger slope, i.e., a larger spatial-contention diversity. Such results are in line with the Corollaries presented in the previous subsections. All the observations shown in this section clearly exhibit the advantages of seeking cooperation in vehicular communication networks, under Weibull fading and random interference, and also provide explicit connections between the performance of CVC and system parameters.

VI. CONCLUSION

We have investigated the performance in a three-node relay-assisted V2V communication network driving on a highway road, under Weibull block fading and one-dimensional Poisson field of interference. We have exploited Weibull PDF approximation and stochastic geometry to analyze the complex impacts of random interference and fading phenomenon. By this means, approximation expressions of the successful transmission probability and error probability of both direct source-destination transmission and cooperative vehicular communication have been attained. Extensive Monte-Carlo simulations have been conducted to validate the accuracy of our results, and demonstrated the strength of cooperative vehicular networking. Our methods and results can potentially be applied to facilitate stochastic geometric analysis in other complex wireless networks under Weibull fading.

APENDIX A
PROOF OF PROPOSITION 2

Since $\mathbb{P}_{\text{suc}} = \Pr\{\text{SINR}_{SD}^{[1]} > T\} - \Pr\{\text{SINR}_{SD}^{[1]} > T, \text{SINR}_{SR}^{[1]} > T\} + \Pr\{\text{SINR}_{SR}^{[1]} > T, \text{SINR}_{\text{MRC}} > T\}$, we derive the three terms individually.

First, setting $a = S$ and $b = D$ in (12) leads to $\Pr\{\text{SINR}_{SD}^{[1]} > T\} \approx \sum_{j=1}^{M} \frac{\beta_j}{p_j} e^{-p_j T d_{SD}^{\alpha} \eta^{-1}} \mathcal{L}_{I_D^{[i]}}(p_j T d_{SD}^{\alpha})$.

Because the events $\text{SINR}_{SR}^{[1]} > T$ and $\text{SINR}_{SD}^{[1]} > T$ are conditionally independent for any given Φ_i, we have $\Pr\{\text{SINR}_{SR}^{[1]} > T, \text{SINR}_{SD}^{[1]} > T \big| \Phi_1\} = \Pr\{\text{SINR}_{SR}^{[1]} > T \big| \Phi_1\} \cdot \Pr\{\text{SINR}_{SD}^{[1]} > T \big| \Phi_1\}$. From (13), we can obtain

$$\begin{aligned}
&\Pr\{\text{SINR}_{SR}^{[1]} > T \big| \Phi_1\} \\
&\approx \sum_{j=1}^{M} \frac{\beta_j}{p_j} \mathbb{E}_{\boldsymbol{h}_R^{[1]}}\left[e^{-p_j \psi_3 (I_R^{[i]} + \eta^{-1})} \big| \Phi_1\right] \\
&= \sum_{j=1}^{M} \frac{\beta_j}{p_j} e^{-\frac{p_j \psi_3}{\eta}} \prod_{x_i \in \Phi_1} \mathbb{E}_h\left[e^{-p_j \psi_3 h |x_i - x_r|^{-\alpha}}\right], \qquad (27)
\end{aligned}$$

where h is a Weibull distributed random variable with parameters k and ρ, and $\psi_3 = T d_{SR}^{\alpha}$. Similarly,

$$\begin{aligned}
&\Pr\{\text{SINR}_{SD}^{[1]} > T \big| \Phi_1\} \\
&\qquad \approx \sum_{j=1}^{M} \frac{\beta_j}{p_j} e^{-\frac{p_j T d_{SD}^{\alpha}}{\eta}} \prod_{x_i \in \Phi_1} \mathbb{E}_h\left[e^{-p_j T d_{SD}^{\alpha} h |x_i|^{-\alpha}}\right].
\end{aligned}$$

From the above two expressions, we can have

$$\begin{aligned}
&\Pr\{\text{SINR}_{SR}^{[1]} > T, \text{SINR}_{SD}^{[1]} > T\} \\
&= \mathbb{E}_{\Phi_1}\left[\Pr\{\text{SINR}_{SR}^{[1]} > T | \Phi_1\} \cdot \Pr\{\text{SINR}_{SD}^{[1]} > T | \Phi_1\}\right] \\
&\approx \sum_{l=1}^{M} \sum_{j=1}^{M} \frac{\beta_l \beta_j}{p_l p_j} e^{-p_l T d_{SR}^{\alpha} \eta^{-1} - p_j T d_{SD}^{\alpha} \eta^{-1}} \\
&\quad \times \mathbb{E}_{\Phi_1}\left[\prod_{x_i \in \Phi_1} \mathbb{E}_h\left[e^{-\frac{p_l T d_{SR}^{\alpha} h}{|x_i - x_r|^{\alpha}}}\right] \mathbb{E}_h\left[e^{-\frac{p_j T d_{SD}^{\alpha} h}{|x_i|^{\alpha}}}\right]\right], \qquad (28)
\end{aligned}$$

with

$$\begin{aligned}
&\mathbb{E}_{\Phi_1}\left[\prod_{x_i \in \Phi_1} \mathbb{E}_h\left[e^{-\frac{v_2 h}{|x_i - x_r|^{\alpha}}}\right] \mathbb{E}_h\left[e^{-\frac{v_1 h}{|x_i|^{\alpha}}}\right]\right] \\
&\overset{(a)}{=} \exp\Bigg(-\lambda\tau \underbrace{\int_{\mathbb{R}} \left(1 - \mathbb{E}_h\left[e^{-\frac{v_2 h}{|x - x_r|^{\alpha}}}\right] \mathbb{E}_h\left[e^{-\frac{v_1 h}{|x|^{\alpha}}}\right]\right) \mathrm{d}x}_{\mathcal{I}}\Bigg),
\end{aligned}$$

where (a) follows from applying the PGFL of PPP [34]. Clearly, the integral $\mathcal{I} = \mathcal{G}_1 + \mathcal{G}_2 - \mathcal{G}_3$, where

$$\begin{aligned}
\mathcal{G}_1 &= \int_{\mathbb{R}} \left(1 - \mathbb{E}_h\left[e^{-\frac{v_1 h}{|x|^{\alpha}}}\right]\right) dx \overset{(a)}{=} 2(\rho v_1)^{1/\alpha} C_{\alpha,k}, \\
\mathcal{G}_2 &= \int_{\mathbb{R}} \left(1 - \mathbb{E}_h\left[e^{-\frac{v_2 h}{|x - x_r|^{\alpha}}}\right]\right) dx = 2(\rho v_2)^{1/\alpha} C_{\alpha,k}, \\
\mathcal{G}_3 &= \int_{\mathbb{R}} \left(1 - \mathbb{E}_h\left[e^{-\frac{v_1 h}{|x|^{\alpha}}}\right]\right)\left(1 - \mathbb{E}_h\left[e^{-\frac{v_2 h}{|x - x_r|^{\alpha}}}\right]\right) \mathrm{d}x \\
&\overset{(b)}{\approx} \sum_{i=1}^{M} \sum_{j=1}^{M} \frac{\beta_i \beta_j}{p_i p_j} \mathcal{I}_0\left(\frac{p_i}{v_1}, \frac{p_j}{v_2}\right),
\end{aligned}$$

step (a) follows from using the same approach in [34, pp. 103], and step (b) follows from (10) and the fact $\sum_{i=1}^{M} \beta_i / p_i = 1$. Hence, with the definition (20) we obtain

$$\mathbb{E}_{\Phi_1}\left[\prod_{x_i \in \Phi_1} \mathbb{E}_h\left[e^{-\frac{v_2 h}{|x_i - x_r|^{\alpha}}}\right] \mathbb{E}_h\left[e^{-\frac{v_1 h}{|x_i|^{\alpha}}}\right]\right] \approx e^{-\lambda\tau \mathcal{I}_1(v_1, v_2)}. \qquad (29)$$

Combining (28) and (29) leads to the expression of $\Pr\{\mathrm{SINR}_{SR}^{[1]} > T, \mathrm{SINR}_{SD}^{[1]} > T\}$ as the second term of (24).

Finally, regarding $\Pr\{\mathrm{SINR}_{SR}^{[1]} > T, \mathrm{SINR}_{\mathrm{MRC}} > T\}$, since the events $\mathrm{SINR}_{SR}^{[1]} > T$ and $\mathrm{SINR}_{\mathrm{MRC}} > T$ are conditionally independent for given Φ_1, we have $\Pr\{\mathrm{SINR}_{SR}^{[1]} > T, \mathrm{SINR}_{\mathrm{MRC}} > T|\Phi_1\} = \Pr\{\mathrm{SINR}_{SR}^{[1]} > T|\Phi_1\} \cdot \Pr\{\mathrm{SINR}_{\mathrm{MRC}} > T|\Phi_1\}$. In order to compute $\Pr\{\mathrm{SINR}_{\mathrm{MRC}} \geq T|\Phi_1\}$, let $Z = \mathrm{SINR}_{RD}^{[2]}$ and $Y_D^{[1]} = I_D^{[1]} + \eta^{-1}$. We have

$$\begin{aligned}
&\Pr\{\mathrm{SINR}_{SD}^{[1]} > T - Z|\Phi_1, Z\} \\
&= \mathbb{E}_{\boldsymbol{h}_D^{[1]}}\Big[\Pr\{h_{SD} > (T-Z)Y_D^{[1]}|\Phi_1, Z\}\Big] \\
&\overset{(a)}{\approx} \sum_{i=1}^{M} \frac{\beta_i}{p_i} \mathbb{E}_{\boldsymbol{h}_D^{[1]}}\Big[\exp\big(-p_i d_{SD}^{\alpha}(T-Z)^{+}Y_D^{[1]}\big)\Big],
\end{aligned}$$

where (a) follows from (11). In addition,

$$\begin{aligned}
&\frac{\mathrm{d}}{\mathrm{d}z}\Pr\{Z < z|\Phi_1\} \\
&= \frac{\mathrm{d}}{\mathrm{d}z}\mathbb{E}_{\boldsymbol{h}_D^{[1]}}\Big[\Pr\{h_{RD} < z d_{RD}^{\alpha} Y_D^{[1]}|\Phi_1\}\Big] \\
&\overset{(a)}{\approx} \frac{\mathrm{d}}{\mathrm{d}z}\Big(1 - \sum_{i=1}^{M} \frac{\beta_i}{p_i}\mathbb{E}_{\boldsymbol{h}_D^{[1]}}\Big[\exp\big(-z p_i d_{RD}^{\alpha} Y_D^{[1]}\big)\Big]\Big) \\
&= \sum_{i=1}^{M} \frac{\beta_i}{p_i}\mathbb{E}_{\boldsymbol{h}_D^{[1]}}\Big[p_i d_{RD}^{\alpha} Y_D^{[1]} \exp\big(-z p_i d_{RD}^{\alpha} Y_D^{[1]}\big)\Big] \\
&= -\sum_{i=1}^{M} \frac{\beta_i}{p_i} z^{-1}\mathbb{E}_{\boldsymbol{h}_D^{[1]}}\Big[\frac{\mathrm{d}}{\mathrm{d}s} e^{-s z p_i d_{RD}^{\alpha} Y_D^{[1]}}\Big|_{s=1}\Big],
\end{aligned}$$

where (a) also follows from (11). Now we have

$$\begin{aligned}
&\Pr\{\mathrm{SINR}_{\mathrm{MRC}} > T|\Phi_1\} \\
&= \int_0^{\infty} \Pr\{\mathrm{SINR}_{SD}^{[1]} > T - z|\Phi_1\} \cdot \frac{\mathrm{d}}{\mathrm{d}z}\Pr\{Z < z|\Phi_1\}\,\mathrm{d}z \\
&\overset{(a)}{\approx} -\sum_{i=1}^{M}\sum_{j=1}^{M} \frac{\beta_i\beta_j}{p_i p_j} \int_{\mathbb{R}} \frac{\mathrm{d}}{z\mathrm{d}s}\Big[\exp\Big(-\frac{p_i\psi_1 + s p_j \psi_2}{\eta}\Big) \\
&\quad \times \prod_{x_i \in \Phi_1} \mathbb{E}_h\Big[e^{-\frac{(p_i\psi_1 + s p_j\psi_2)h}{|x_i|^{\alpha}}}\Big]\Big]\Big|_{s=1} \mathrm{d}z. \qquad (30)
\end{aligned}$$

where in (a) we substitute $\psi_1 = d_{SD}^{\alpha}(T-z)^{+}$, $\psi_2 = z d_{RD}^{\alpha}$. Combining (27) and (30), we can obtain

$$\begin{aligned}
&\Pr\{\mathrm{SINR}_{SR}^{[1]} > T, \mathrm{SINR}_{\mathrm{MRC}} > T\} \\
&= \mathbb{E}_{\Phi_1}\big[\Pr\{\mathrm{SINR}_{\mathrm{SR}}^{[1]} > T|\Phi_1\} \cdot \Pr\{\mathrm{SINR}_{\mathrm{MRC}} > T|\Phi_1\}\big] \\
&\approx -\sum_{l=1}^{M}\sum_{i=1}^{M}\sum_{j=1}^{M} \frac{\beta_l\beta_i\beta_j}{p_l p_i p_j} \int_{\mathbb{R}} \frac{\mathrm{d}}{z\mathrm{d}s}\Big[e^{-\frac{p_i\psi_1 + s p_j\psi_2 + p_l\psi_3}{\eta}} \\
&\quad \times \mathbb{E}_{\Phi_1}\Big[\prod_{x_i \in \Phi_1} \mathbb{E}_h\Big[e^{-\frac{(p_i\psi_1 + s p_j\psi_2)h}{|x_i|^{\alpha}}}\Big]\mathbb{E}_h\Big[e^{-\frac{p_l\psi_3 h}{|x_i - x_r|^{\alpha}}}\Big]\Big]\Big]\Big|_{s=1} \mathrm{d}z.
\end{aligned}$$

Applying (29) yields the third term of (24).

The proof of Proposition 2 now completes.

APPENDIX B
PROOF OF COROLLARY 1

Weibull PDF $f_h(x;\rho,k)$ for $k < 1$ is completely monotone, since $(-1)^n \frac{\mathrm{d}^n}{\mathrm{d}x^n} f_h(x;\rho,k) \geq 0$ for all $x > 0$ and $n \geq 1$. Such a characteristic of PDF yields positive β_i and p_i in (10) for all $i \in \{1, 2, \cdots, M\}$ [44]. For presentation simplicity, define $\mathbb{P}_2 = \Pr\{\mathrm{SINR}_{SR}^{[1]} > T, \mathrm{SINR}_{SD}^{[1]} > T\}$, and $\mathbb{P}_3 = \Pr\{\mathrm{SINR}_{SR}^{[1]} > T, \mathrm{SINR}_{\mathrm{MRC}} > T\}$. Then the system error probability $\mathbb{P}_{\mathrm{err}} = 1 - \Pr\{\mathrm{SINR}_{SD}^{[1]} > T\} + \mathbb{P}_2 - \mathbb{P}_3$. Because $\mathrm{SINR}_{\mathrm{MRC}} \geq \mathrm{SINR}_{SD}^{[1]}$, the following inequality holds

$$\mathbb{P}_2 \leq \mathbb{P}_3 \leq \Pr\Big\{\mathrm{SINR}_{SR}^{[1]} > T\Big\}.$$

Therefore, we have

$$\varpi_1(\lambda\tau) \leq \mathbb{P}_{\mathrm{err}} \leq \varpi_2(\lambda\tau),$$

where $\varpi_1(\lambda\tau) = 1 - \Pr\{\mathrm{SINR}_{SD}^{[1]} > T\} - \Pr\{\mathrm{SINR}_{SR}^{[1]} > T\} + \mathbb{P}_2$, and $\varpi_2(\lambda\tau) = 1 - \Pr\{\mathrm{SINR}_{SD}^{[1]} > T\}$. As $\lambda\tau \to 0$, $\eta \to \infty$, and $M \to \infty$, Proposition 1 results in

$$\Pr\{\mathrm{SINR}_{SD}^{[1]} > T\} \to 1 - A_1\lambda\tau,$$

where $A_1 = 2\, C_{\alpha,k}(\rho T d_{SD}^{\alpha})^{1/\alpha} \sum_{j=1}^{\infty} \frac{\beta_j}{p_j^{1-1/\alpha}} > 0$. Hence $\varpi_2(\lambda\tau) \to A_1\lambda\tau$. Similarly, we have

$$\Pr\Big\{\mathrm{SINR}_{SR}^{[1]} > T\Big\} \to 1 - A_2\lambda\tau,$$

where $A_2 = 2\, C_{\alpha,k}(\rho T d_{SR}^{\alpha})^{1/\alpha} \sum_{j=1}^{\infty} \frac{\beta_j}{p_j^{1-1/\alpha}}$. And

$$\begin{aligned}
\mathbb{P}_2 &\to 1 - \lambda\tau \sum_{i=1}^{\infty}\sum_{j=1}^{\infty} \frac{\beta_i\beta_j}{p_i p_j} \mathcal{I}_1\big(p_i T d_{SR}^{\alpha}, p_j T d_{SD}^{\alpha}\big) \\
&\overset{(a)}{=} 1 - (A_1 + A_2 - A_3)\lambda\tau,
\end{aligned}$$

where in step (a) we use (20), with

$$A_3 = \sum_{i=1}^{\infty}\sum_{j=1}^{\infty}\sum_{l=1}^{\infty}\sum_{m=1}^{\infty} \frac{\beta_i\beta_j\beta_l\beta_m}{p_i p_j p_l p_m} \mathcal{I}_0\Big(\frac{p_l}{p_i T d_{SR}^{\alpha}}, \frac{p_m}{p_j T d_{SD}^{\alpha}}\Big).$$

Obviously, $A_3 > 0$, because $\beta_i > 0$, $p_i > 0$ for all i, and $\mathcal{I}_0(\sigma_1, \sigma_2) > 0$ for positive σ_1 and σ_2. As a result, $\varpi_1(\lambda\tau) \to A_3\lambda\tau$. If d_{SR} does not tend to 0, then A_3 does not tend to 0. Recall that $\varpi_2(\lambda\tau) \to A_1\lambda\tau$. Thus $\mathbb{P}_{\mathrm{err}} = \Theta(\lambda\tau)$.

On the other hand, when $d_{SR} \to 0$, we have $A_3 \to 0$ because $\mathcal{I}_0(\sigma_1, \sigma_2) \to 0$ when $\sigma_1 \to \infty$. In this case, we resort to (24) by setting $d_{SR} \to 0$. Now R can recover the source message with probability 1. Then $\mathbb{P}_2 \to \Pr\{\mathrm{SINR}_{SD}^{[1]} > T\}$, and $\mathbb{P}_3 \to \Pr\{\mathrm{SINR}_{\mathrm{MRC}} > T\}$. Hence

$$\begin{aligned}
\mathbb{P}_{\mathrm{err}} &= 1 - \Pr\{\mathrm{SINR}_{SD}^{[1]} > T\} + \mathbb{P}_2 - \mathbb{P}_3 \\
&\to 1 - \Pr\{\mathrm{SINR}_{\mathrm{MRC}} > T\} \\
&\overset{(a)}{\to} 1 + \sum_{i=1}^{\infty}\sum_{j=1}^{\infty} \frac{\beta_i\beta_j}{p_i p_j} \int_0^{\infty} \frac{\mathrm{d}}{z\mathrm{d}s} e^{-\lambda\tau\mathcal{I}_1(0, p_i\psi_1 + s p_j\psi_2)}\Big|_{s=1} \mathrm{d}z,
\end{aligned}$$

where in step (a) we take $\eta \to 0$, $\psi_3 = T d_{SR}^{\alpha} \to 0$ for the third term of (24), and use the fact that $\sum_{l=1}^{\infty} \frac{\beta_l}{p_l} = 1$.

The integral in the last line can be decomposed into the sum of two integrals. The first integral is expressed as

$$\begin{aligned}
&\int_0^T \frac{\mathrm{d}}{z\mathrm{d}s} e^{-\lambda\tau\mathcal{I}_1(0,p_i\psi_1+sp_j\psi_2)}\Big|_{s=1}\mathrm{d}z \\
&\overset{(a)}{\to} \int_0^T \frac{\mathrm{d}}{z\mathrm{d}s}\big(1-\lambda\tau\mathcal{I}_1(0,p_i\psi_1+sp_j\psi_2)\big)\Big|_{s=1}\mathrm{d}z \\
&\overset{(b)}{=} \int_0^T \frac{\mathrm{d}}{z\mathrm{d}s}\big(1-2\lambda\tau\rho^{\frac{1}{\alpha}}C_{\alpha,k}(p_i\psi_1+sp_j\psi_2)^{\frac{1}{\alpha}}\big)\Big|_{s=1}\mathrm{d}z \\
&\overset{(c)}{\to} -\frac{A_4 p_j\lambda\tau}{\alpha T^{1/\alpha}}\int_0^T (p_i(T-z)+p_j z)^{-1+1/\alpha}\mathrm{d}z,
\end{aligned}$$

where in (a), we apply the Taylor expansion $e^{-x}\to 1-x$ for $x\to 0$, in (b) we use (20), and step (c) follows from $d_{RD}\to d_{SD}$, with $A_4=2(\rho T)^{1/\alpha}C_{\alpha,k}d_{SD}>0$. The second integral is given by

$$\begin{aligned}
&\int_T^\infty \frac{\mathrm{d}}{z\mathrm{d}s} e^{-\lambda\tau\mathcal{I}_1(0,p_i\psi_1+sp_j\psi_2)}\Big|_{s=1}\mathrm{d}z \\
&\overset{(a)}{=} \int_T^\infty \frac{\mathrm{d}}{z\mathrm{d}s} e^{-\lambda\tau\mathcal{I}_1(0,sp_j\psi_2)}\Big|_{s=1}\mathrm{d}z \\
&= \int_T^\infty \frac{\mathrm{d}}{z\mathrm{d}s} e^{-2\lambda\tau C_{\alpha,k}d_{RD}(p_j\rho sz)^{1/\alpha}}\Big|_{s=1}\mathrm{d}z \\
&= -e^{-2\lambda\tau C_{\alpha,k}d_{RD}(p_j\rho T)^{1/\alpha}} \\
&\overset{(b)}{\to} -1+A_4 p_j^{1/\alpha}\lambda\tau,
\end{aligned}$$

where in step (a) we use the fact that $\psi_2=zd_{RD}^\alpha=0$, and in step (b) we use the Taylor expansion and take $d_{RD}\to d_{SD}$. Therefore, we have $\mathbb{P}_{\mathrm{err}}\to A_4\,A_5\lambda\tau$ when $d_{SR}\to 0$, with

$$\begin{aligned}
A_5 &= \sum_{i=1}^M\sum_{j=1}^M \frac{\beta_i\beta_j}{p_ip_j}\Big(p_j^{\frac{1}{\alpha}}-\frac{p_j\int_0^T(p_i(T-z)+p_jz)^{-1+\frac{1}{\alpha}}\mathrm{d}z}{\alpha T^{1/\alpha}}\Big) \\
&> \sum_{i=1}^M\sum_{j=1}^M \frac{\beta_i\beta_j}{p_ip_j}\Big(p_j^{\frac{1}{\alpha}}-\frac{p_j\int_0^T(p_jz)^{-1+\frac{1}{\alpha}}\mathrm{d}z}{\alpha T^{1/\alpha}}\Big)=0.
\end{aligned}$$

Hence $\mathbb{P}_{\mathrm{err}}=\Theta(\lambda\tau)$ when $d_{SR}\to 0$.

From the above results, we can conclude $\mathbb{P}_{\mathrm{err}}=\Theta(\lambda\tau)$.

APENDIX C
PROOF OF PROPOSITION 3

The proof process is similar to that for Proposition 2. The probability $\mathbb{P}_{\mathrm{suc}}$ in (4) can be expressed as the summation of three probabilities: $\mathbb{P}_{\mathrm{suc}}=\Pr\{\mathrm{SINR}_{SD}>T\}-\Pr\{\mathrm{SINR}_{SR}^{[1]}>T,\mathrm{SINR}_{SD}^{[1]}>T\}+\Pr\{\mathrm{SINR}_{SR}^{[1]}>T,\mathrm{SINR}_{\mathrm{MRC}}>T\}$. Approximation expressions of the first two can be found follow the proofs of Propositions 1 and 2. Hence we focus only on the last term.

Conditioning on Φ_1 and Φ_2, the events $\mathrm{SINR}_{SR}^{[1]}>T$ and $\mathrm{SINR}_{\mathrm{MRC}}>T$ are independent, i.e., $\Pr\{\mathrm{SINR}_{SR}^{[1]}>T,\mathrm{SINR}_{\mathrm{MRC}}>T\big|\Phi_1,\Phi_2\}=\Pr\{\mathrm{SINR}_{SR}^{[1]}>T\big|\Phi_1\}\cdot\Pr\{\mathrm{SINR}_{\mathrm{MRC}}>T\big|\Phi_1,\Phi_2\}$. The approximation to $\Pr\{\mathrm{SINR}_{SR}^{[1]}>T|\Phi_1\}$ is given in (27). Similar to Appendix A, $\Pr\{\mathrm{SINR}_{\mathrm{MRC}}>T|\Phi_1,\Phi_2\}$ can be expressed as

$$\begin{aligned}
&\Pr\{\mathrm{SINR}_{\mathrm{MRC}}\ge T|\Phi_1,\Phi_2\} \\
&= \int_0^\infty \Pr\{\mathrm{SINR}_{SD}^{[1]}\ge T-z|\Phi\}\cdot\frac{\mathrm{d}}{\mathrm{d}z}\Pr\{Z<z|\Phi\}\,\mathrm{d}z \\
&\overset{(a)}{=} -\sum_{i=1}^M\sum_{j=1}^M\frac{\beta_i\beta_j}{p_ip_j}\int_{\mathbb{R}}\frac{\mathrm{d}}{z\mathrm{d}s}\Big[\exp\Big(-\frac{p_i\psi_1+sp_j\psi_2}{\eta}\Big) \\
&\quad\times\prod_{x_i\in\Phi_1}\mathbb{E}_h\Big[e^{-\frac{p_i\psi_1 h}{|x_i|^\alpha}}\Big]\prod_{x_i\in\Phi_2}\mathbb{E}_h\Big[e^{-\frac{sp_j\psi_2 h}{|x_i|^\alpha}}\Big]\Big]\Big|_{s=1}\mathrm{d}z. \qquad (31)
\end{aligned}$$

where we substitute $\psi_1=d_{SD}^\alpha(T-z)^+$, $\psi_2=zd_{RD}^\alpha$ in step (a). The original unconditional joint probability therefore is

$$\begin{aligned}
&\Pr\{\mathrm{SINR}_{SR}^{[1]}>T,\mathrm{SINR}_{\mathrm{MRC}}>T\} \\
&= \mathbb{E}\big[\Pr\{\mathrm{SINR}_{\mathrm{SR}}^{[1]}>T|\Phi_1\}\cdot\Pr\{\mathrm{SINR}_{\mathrm{MRC}}>T|\Phi_1,\Phi_2\}\big] \\
&\approx -\sum_{l=1}^M\sum_{i=1}^M\sum_{j=1}^M\frac{\beta_l\beta_i\beta_j}{p_lp_ip_j}\int_{\mathbb{R}}\frac{\mathrm{d}}{z\mathrm{d}s}\Big[e^{-\frac{p_i\psi_1+sp_j\psi_2+p_l\psi_3}{\eta}} \\
&\quad\times\mathbb{E}\Big\{\prod_{x_i\in\Phi_1}\mathbb{E}_h\Big[e^{-\frac{p_i\psi_1 h}{|x_i|^\alpha}}\Big]\mathbb{E}_h\Big[e^{-\frac{p_l\psi_3 h}{|x_i-x_r|^\alpha}}\Big] \\
&\quad\times\prod_{x_i\in\Phi_2}\mathbb{E}_h\Big[e^{-\frac{sp_j\psi_2 h}{|x_i|^\alpha}}\Big]\Big\}\Big]\Big|_{s=1}\mathrm{d}z, \qquad (32)
\end{aligned}$$

where

$$\begin{aligned}
&\mathbb{E}\Big[\prod_{x_i\in\Phi_1}\mathbb{E}_h\Big[e^{-\frac{v_1 h}{|x_i|^\alpha}}\Big]\mathbb{E}_h\Big[e^{-\frac{v_3 h}{|x_i-x_r|^\alpha}}\Big]\prod_{x_i\in\Phi_2}\mathbb{E}_h\Big[e^{-\frac{v_2 h}{|x_i|^\alpha}}\Big]\Big] \\
&\qquad\overset{(a)}{=}\exp\Big(-\lambda\underbrace{\int_{\mathbb{R}}\Big(1-\epsilon_1(x)\epsilon_2(x)\,\mathrm{d}x\Big)}_{\mathcal{I}'}\Big), \qquad (33)
\end{aligned}$$

with step (a) following from the PGFL of PPP [34], $\epsilon_1(x)=1-\tau+\tau\mathbb{E}_h\Big[e^{-\frac{v_1 h}{|x|^\alpha}}\Big]\mathbb{E}_h\Big[e^{-\frac{v_3 h}{|x-x_r|^\alpha}}\Big]$, and $\epsilon_2(x)=1-\tau+\tau\mathbb{E}_h\Big[e^{-\frac{v_2 h}{|x|^\alpha}}\Big]$. The integral $\mathcal{I}'$ can be written as $\mathcal{I}'=\tau(1-\tau)\mathcal{G}_1'+\tau(1-\tau)\mathcal{G}_2'+\tau^2\mathcal{G}_3'$, with

$$\begin{aligned}
\mathcal{G}_1' &= \int_{\mathbb{R}}\Big(1-\mathbb{E}_h\Big[e^{-\frac{-v_1 h}{|x|^\alpha}}\Big]\mathbb{E}_h\Big[e^{-\frac{-v_3 h}{|x-x_r|^\alpha}}\Big]\Big)\mathrm{d}x\overset{(a)}{=}\mathcal{I}_1(v_1,v_3), \\
\mathcal{G}_2' &= \int_{\mathbb{R}}\Big(1-\mathbb{E}_h\Big[e^{-\frac{-v_2 h}{|x|^\alpha}}\Big]\Big)\,\mathrm{d}x=2(\rho v_2)^{1/\alpha}C_{\alpha,k}, \\
\mathcal{G}_3' &= \int_{\mathbb{R}}\Big(1-\mathbb{E}_h[e^{-\frac{-v_1 h}{|x|^\alpha}}]\mathbb{E}_h[e^{-\frac{-v_2 h}{|x|^\alpha}}]\mathbb{E}_h[e^{-\frac{-v_3 h}{|x-x_r|^\alpha}}]\Big)\mathrm{d}x \\
&\overset{(b)}{\approx}\sum_{l=1}^M\sum_{i=1}^M\sum_{j=1}^M\frac{\beta_l\beta_i\beta_j}{p_lp_ip_j}\int_{\mathbb{R}}\Big(1-\frac{1}{1+p_i^{-1}v_1|x|^{-\alpha}} \\
&\quad\cdot\frac{1}{1+p_j^{-1}v_2|x|^{-\alpha}}\cdot\frac{1}{1+p_l^{-1}v_3|x-x_r|^{-\alpha}}\Big)\,\mathrm{d}x,
\end{aligned}$$

where step (a) follows from (29), and in step (b) we use (10) three times as well as the fact that $\sum_{i=1}^M\frac{\beta_i}{p_i}=1$. The integral

contained in $\mathcal{G}_3'$ can be obtained as

$$\begin{aligned}
&\int_{\mathbb{R}} \Big(1 - \frac{1}{(1+\frac{s_1}{|x|^\alpha})(1+\frac{s_2}{|x|^\alpha})(1+\frac{s_3}{|x-x_r|^\alpha})}\Big)\,\mathrm{d}x \\
&= \frac{s_1}{s_1-s_2}\int_{\mathbb{R}} \Big(1 - \frac{1}{(1+\frac{s_1}{|x|^\alpha})(1+\frac{s_3}{|x-x_r|^\alpha})}\Big)\,\mathrm{d}x \\
&\quad - \frac{s_2}{s_1-s_2}\int_{\mathbb{R}} \Big(1 - \frac{1}{(1+\frac{s_2}{|x|^\alpha})(1+\frac{s_3}{|x-x_r|^\alpha})}\Big)\,\mathrm{d}x \\
&\overset{(a)}{=} \mathcal{I}_2(s_1, s_2, s_3),
\end{aligned}$$

where in step (a) we use (22). Therefore, we have $\mathcal{I}' \approx \mathcal{I}_3(v_1, v_2, v_3)$. Substituting these results into (32) results in the approximation for $\Pr\{\mathrm{SINR}_{SR}^{[1]} > T, \mathrm{SINR}_{\mathrm{MRC}} > T\}$. All the above approximations are summarized in (26). The proof of Proposition 3 now completes.

APENDIX D
PROOF OF COROLLARY 2

The proof follows the similar procedure as Appendix B. We can also distinguish the two cases: whether $d_{SR} \to 0$ holds or not. For the latter case, the method presented in Appendix B can be directly applied to reach $\mathbb{P}_{\mathrm{err}} = \Theta(\lambda\tau)$. Hence we focus only on the situation $d_{SR} \to 0$.

When $\lambda\tau \to 0$, and $\eta \to \infty$, using (26) we can have

$$\begin{aligned}
\mathbb{P}_{\mathrm{err}} &= 1 - \Pr\{\mathrm{SINR}_{\mathrm{MRC}} > T\} \\
&\overset{(a)}{\to} 1 + \sum_{i=1}^{\infty}\sum_{j=1}^{\infty} \frac{\beta_i\beta_j}{p_i p_j} \int_0^{\infty} \frac{\mathrm{d}}{z\mathrm{d}s} e^{-\lambda\mathcal{I}_3(p_i\psi_1, sp_j\psi_2, 0)}\Big|_{s=1} \mathrm{d}z.
\end{aligned}$$

where in step (a) we take $\psi_3 = Td_{SR}^{\alpha} \to 0$, and use the fact that $\sum_{l=1}^{\infty}\frac{\beta_l}{p_l} = 1$. The integral in the last line can be decomposed into the sum of two integrals. The first is

$$\begin{aligned}
&\int_0^T \frac{\mathrm{d}}{z\mathrm{d}s} e^{-\lambda\mathcal{I}_3(p_i\psi_1, sp_j\psi_2, 0)}\Big|_{s=1} \mathrm{d}z \\
&\overset{(a)}{\to} \int_0^T \frac{\mathrm{d}}{z\mathrm{d}s}\Big(1 - \lambda\mathcal{I}_3(p_i\psi_1, sp_j\psi_2, 0) + \frac{(A_4\lambda\tau)^2(sz)^{\frac{2}{\alpha}}}{2(p_j^{-1}T)^{\frac{2}{\alpha}}}\Big)\Big|_{s=1}\mathrm{d}z \\
&\overset{(b)}{\to} -A_4 p_j^{\frac{1}{\alpha}}\lambda\tau + (A_4 p_j^{\frac{1}{\alpha}}\lambda\tau)^2/2 + B\lambda\tau^2,
\end{aligned}$$

where in (a), we use the Taylor expansion $e^{-x} \to 1 - x + x^2/2$ for $x \to 0$, and ignore the terms which are higher than $\lambda\tau^2$ and $(\lambda\tau)^2$, and in (b) we use the definition of $\mathcal{I}'$ in (33) and the fact that $\mathcal{I}' = \mathcal{I}_3(v_1, v_2, v_3)$ as $M \to \infty$, with

$$B = \int_0^T \int_{\mathbb{R}} \frac{\mathrm{d}\mathbb{E}_h\big[e^{-\frac{-sp_j\psi_2 h}{|x|^\alpha}}\big]}{z\mathrm{d}s}\Big|_{s=1} \Big(\mathbb{E}_h\big[e^{-\frac{-p_i\psi_1 h}{|x|^\alpha}}\big] - 1\Big)\mathrm{d}x\mathrm{d}z$$

being a positive number. The second integral is given by

$$\begin{aligned}
&\int_T^{\infty} \frac{\mathrm{d}}{z\mathrm{d}s} e^{-\lambda\mathcal{I}_3(p_i\psi_1, sp_j\psi_2, 0)}\Big|_{s=1} \mathrm{d}z \\
&= \int_T^{\infty} \frac{\mathrm{d}}{z\mathrm{d}s} e^{-\lambda\mathcal{I}_3(0, sp_j\psi_2, 0)}\Big|_{s=1} \mathrm{d}z \\
&\overset{(a)}{\to} \int_T^{\infty} \frac{\mathrm{d}}{z\mathrm{d}s} e^{-(sz)^{1/\alpha}\left(A_4 p_j^{1/\alpha} T^{-1/\alpha}\lambda\tau\right)}\Big|_{s=1} \mathrm{d}z \\
&\overset{(b)}{=} -e^{-A_4 p_j^{1/\alpha}\lambda\tau} \\
&\overset{(c)}{\to} -1 + A_4 p_j^{1/\alpha}\lambda\tau - (A_4 p_j^{1/\alpha}\lambda\tau)^2/2,
\end{aligned}$$

where in (a) we use (33), in (b) we evaluate the integral directly, and in (c) we use the Taylor expansion. Therefore, $\mathbb{P}_{\mathrm{err}} = \Theta(\lambda\tau^2)$ when $d_{SR} \to 0$. These complete the proof.

ACKNOWLEDGMENT

This work reflects only the authors' view and the EU Commission is not responsible for any use that may be made of the information it contains.

REFERENCES

[1] Z. MacHardy, A. Khan, K. Obana, and S. Iwashina, "V2X access technologies: Regulation, research, and remaining challenges," *IEEE Commun. Surveys Tuts.*, vol. 20, no. 3, pp. 1858–1877, 3rd Quart., 2018.
[2] M. Whaiduzzaman, M. Sookhak, A. Gani, and R. Buyya, "A survey on vehicular cloud computing," *J. Netw. Comput. Appl.*, vol. 40, pp. 325–344, Apr. 2014.
[3] X. Hou, Y. Li, M. Chen, D. Wu, D. Jin, and S. Chen, "Vehicular fog computing: A viewpoint of vehicles as the infrastructures," *IEEE Trans. Veh. Technol.*, vol. 65, no. 6, pp. 3860–3873, Jun. 2016.
[4] J. B. Kenney, "Dedicated short-range communications (DSRC) standards in the United States," *Proc. IEEE*, vol. 99, no. 7, pp. 1162–1182, Jul. 2011.
[5] S. Subramanian, M. Werner, S. Liu, J. Jose, R. Lupoaie, and X. Wu, "Congestion control for vehicular safety: Synchronous and asynchronous MAC algorithms," in *Proc. ACM Int. Workshop Veh. Inter-Netw., Syst., Appl.*, New York, NY, USA, Jun. 2012, pp. 63–72.
[6] T. V. Nguyen, F. Baccelli, K. Zhu, S. Subramanian, and X. Wu, "A performance analysis of CSMA based broadcast protocol in VANETs," in *Proc. IEEE INFOCOM*, Turin, Italy, Apr. 2013, pp. 2805–2813.
[7] Z. Tong, H. Lu, M. Haenggi, and C. Poellabauer, "A stochastic geometry approach to the modeling of DSRC for vehicular safety communication," *IEEE Trans. Intell. Transp. Syst.*, vol. 17, no. 5, pp. 1448–1458, May 2016.
[8] D. W. Matolak and J. Frolik, "Worse-than-Rayleigh fading: Experimental results and theoretical models," *IEEE Commun. Mag.*, vol. 49, no. 4, pp. 140–146, Apr. 2011.
[9] E. Ahmed and H. Gharavi, "Cooperative vehicular networking: A survey," *IEEE Trans. Intell. Transp. Syst.*, vol. 19, no. 3, pp. 996–1014, Mar. 2018.
[10] J. N. Laneman, D. N. C. Tse, and G. W. Wornell, "Cooperative diversity in wireless networks: Efficient protocols and outage behavior," *IEEE Trans. Inf. Theory*, vol. 50, no. 12, pp. 3062–3080, Dec. 2004.
[11] H. Yu, I.-H. Lee, and G. L. Stuber, "Outage probability of decode-and-forward cooperative relaying systems with co-channel interference," *IEEE Trans. Wireless Commun.*, vol. 11, no. 1, pp. 266–274, Jan. 2012.
[12] J. G. Andrews, F. Baccelli, and R. K. Ganti, "A tractable approach to coverage and rate in cellular networks," *IEEE Trans. Commun.*, vol. 59, no. 11, pp. 3122–3134, Nov. 2011.
[13] V. V. Chetlur and H. S. Dhillon, "Downlink coverage analysis for a finite 3-D wireless network of unmanned aerial vehicles," *IEEE Trans. Commun.*, vol. 65, no. 10, pp. 4543–4558, Jul. 2017.
[14] K. Cho, J. Lee, and C. G. Kang, "Stochastic geometry-based coverage and rate analysis under Nakagami & log-normal composite fading channel for downlink cellular networks," *IEEE Commun. Lett.*, vol. 21, no. 6, pp. 1437–1440, Jun. 2017.
[15] Y. J. Chun, S. L. Cotton, H. S. Dhillon, A. Ghrayeb, and M. O. Hasna, "A stochastic geometric analysis of device-to-device communications operating over generalized fading channels," *IEEE Trans. Wireless Commun.*, vol. 16, no. 7, pp. 4151–4165, Jul. 2017.
[16] R. Tanbourgi, H. S. Dhillon, J. G. Andrews, and F. K. Jondral, "Dual-branch MRC receivers under spatial interference correlation and Nakagami fading," *IEEE Trans. Commun.*, vol. 62, no. 6, pp. 1830–1844, Jun. 2014.
[17] X. Lin, R. Ratasuk, A. Ghosh, and J. G. Andrews, "Modeling, analysis, and optimization of multicast device-to-device transmissions," *IEEE Trans. Wireless Commun.*, vol. 13, no. 8, pp. 4346–4359, Apr. 2014.
[18] R. Tanbourgi, H. Jäkel, and F. K. Jondral, "Cooperative relaying in a Poisson field of interferers: A diversity order analysis," in *Proc. IEEE ISIT*, Istanbul, Turkey, Jul. 2013, pp. 3100–3104.
[19] M. Di Renzo and W. Lu, "End-to-end error probability and diversity analysis of AF-based dual-hop cooperative relaying in a poisson field of interferers at the destination," *IEEE Trans. Wireless Commun.*, vol. 14, no. 1, pp. 15–32, Jan. 2015.

[20] M. Di Renzo and W. Lu, "On the diversity order of selection combining dual-branch dual-hop AF relaying in a Poisson field of interferers at the destination," *IEEE Trans. Veh. Technol.*, vol. 64, no. 4, pp. 1620–1628, Apr. 2015.
[21] J. Lee, H. Shin, I. Lee, and J. Heo, "Optimal linear multihop system for DF relaying in a Poisson field of interferers," *IEEE Commun. Lett.*, vol. 17, no. 11, pp. 2029–2032, Nov. 2013.
[22] V. A. Aalo, G. P. Efthymoglou, T. Soithong, M. Alwakeel, and S. Alwakeel, "Performance analysis of multi-hop amplify-and-forward relaying systems in Rayleigh fading channels with a Poisson interference field," *IEEE Trans. Wireless Commun.*, vol. 13, no. 1, pp. 24–35, Jan. 2014.
[23] A. Crismani, S. Toumpis, U. Schilcher, G. Brandner, and C. Bettstetter, "Cooperative relaying under spatially and temporally correlated interference," *IEEE Trans. Veh. Technol.*, vol. 64, no. 10, pp. 4655–4669, Oct. 2015.
[24] N. Suraweera and N. C. Beaulieu, "Optimum combining for cooperative relaying in a Poisson field of interferers," *IEEE Trans. Commun.*, vol. 63, no. 9, pp. 3132–3142, Sep. 2015.
[25] X. Lai, W. Zou, D. Xie, X. Li, and L. Fan, "DF relaying networks with randomly distributed interferers," *IEEE Access*, vol. 5, pp. 18909–18917, Sep. 2017.
[26] H. Ilhan, M. Uysal, and I. Altunbas, "Cooperative diversity for intervehicular communication: Performance analysis and optimization," *IEEE Trans. Veh. Technol.*, vol. 58, no. 7, pp. 3301–3310, Sep. 2009.
[27] A.-A. A. Boulogeorgos, P. C. Sofotasios, B. Selim, S. Muhaidat, G. K. Karagiannidis, and M. Valkama, "Effects of RF impairments in communications over cascaded fading channels," *IEEE Trans. Veh. Technol.*, vol. 65, no. 11, pp. 8878–8894, Nov. 2016.
[28] C. F. Mecklenbrauker, A. F. Molisch, J. Karedal, F. Tufvesson, A. Paier, L. Bernado, T. Zemen, O. Klemp, and N. Czink, "Vehicular channel characterization and its implications for wireless system design and performance," *Proc. IEEE*, vol. 99, no. 7, pp. 1189–1212, Jul. 2011.
[29] S. S. Ikki and S. Aissa, "A study of optimization problem for amplify-and-forward relaying over weibull fading channels with multiple antennas," *IEEE Commun. Lett.*, vol. 15, no. 11, pp. 1148–1151, Nov. 2011.
[30] M. You, H. Sun, J. Jiang, and J. Zhang, "Effective rate analysis in Weibull fading channels," *IEEE Wireless Commun. Lett.*, vol. 5, no. 4, pp. 340–343, Aug. 2016.
[31] T. H. Cormen, C. E. Leiserson, R. L. Rivest, and C. Stein, *Introduction to Algorithms*. Cambridge, MA, USA: MIT Press, 2009.
[32] V. V. Chetlur and H. S. Dhillon, "Success probability and area spectral efficiency of a VANET modeled as a cox process," *IEEE Wireless Commun. Lett.*, vol. 7, no. 5, pp. 856–859, Oct. 2018.
[33] M. J. Farooq, H. ElSawy, and M.-S. Alouini, "A stochastic geometry model for multi-hop highway vehicular communication," *IEEE Trans. Wireless Commun.*, vol. 15, no. 3, pp. 2276–2291, Mar. 2016.
[34] M. Haenggi, *Stochastic Geometry for Wireless Networks*. Cambridge, U.K.: Cambridge Univ. Press, 2012.
[35] I. Sen and D. W. Matolak, "Vehicle–vehicle channel models for the 5-GHz band," *IEEE Trans. Intell. Transp. Syst.*, vol. 9, no. 2, pp. 235–245, Jun. 2008.
[36] C. M. Harris and W. G. Marchal, "Distribution estimation using Laplace transforms," *Informs J. Comput.*, vol. 10, no. 4, pp. 359–460, 1998.
[37] H. Amindavar and J. A. Ritcey, "Pade approximations of probability density functions," *IEEE Trans. Aerosp. Electron. Syst.*, vol. 30, no. 2, pp. 416–424, Apr. 1994.
[38] N. C. Sagias and G. K. Karagiannidis, "Gaussian class multivariate Weibull distributions: Theory and applications in fading channels," *IEEE Trans. Inf. Theory*, vol. 51, no. 10, pp. 3608–3619, Oct. 2005.
[39] R. F. Botta and C. M. Harris, "Approximation with generalized hyperexponential distributions: Weak convergence results," *Queueing Syst.*, vol. 1, no. 2, pp. 169–190, 1986.
[40] Y. Wang, F. Liu, and P. Wang, "Performance analysis of V2V communications in highway scenarios with Weibull-lognormal composite fading," in *Proc. IEEE WCNC*, Marrakech, Morocco, Apr. 2019, pp. 1–6.
[41] E. Steinmetz, M. Wildemeersch, T. Q. S. Quek, and H. Wymeersch, "A stochastic geometry model for vehicular communication near intersections," in *Proc. IEEE Globecom Workshops*, San Diego, CA, USA, Dec. 2015, pp. 1–6.
[42] J. Brown and R. Churchill, *Complex Variables and Applications*. Boston, MA, USA: McGraw-Hill, 2009.
[43] Y. A. Rahama, M. H. Ismail, and M. S. Hassan, "On the sum of independent fox's H-function variates with applications," *IEEE Trans. Veh. Technol.*, vol. 67, no. 8, pp. 6752–6760, Aug. 2018.
[44] A. Feldmann and W. Whitt, "Fitting mixtures of exponentials to long-tail distributions to analyze network performance models," *Perform. Eval.*, vol. 31, nos. 3–4, pp. 245–279, 1998.

YANG WANG received the B.E. degree in communication engineering from Tongji University, Shanghai, China, in 2014, where he is currently pursuing the Ph.D. degree in control science and engineering. In 2016, he was a Visiting Student with the National Institute of Informatics, The Graduate University for Advanced Studies (SOKENDAI), Tokyo, Japan. His research interests include vehicular networks, resource allocation, and stochastic geometric analysis of wireless networks.

FUQIANG LIU (M'09) received the bachelor's degree from Tianjin University, in 1987, and the Ph.D. degree from the China University of Mining and Technology, in 1996. He is currently a Professor with the School of Electronics and Information Engineering, Tongji University, Shanghai, China. He currently serves as the Director of the Broadband Wireless Communication and Artificial Intelligence Laboratory, Tongji University. He has published more than 300 scientific articles and 9 books. He is the project leader of more than 20 national research projects in China, including high-tech key projects from MOST and key projects from NSF of China. His research interests include information and communications technologies, and innovation applications in automotive and intelligent transportation systems. He has also received research funding from USA, Finland, EU FP7, and Japan.

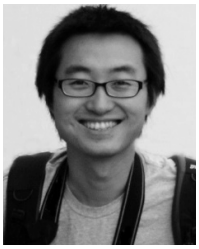

CHAO WANG (S'07–M'09) received the B.E. degree from the University of Science and Technology of China (USTC), Hefei, China, in 2003, and the M.Sc. and Ph.D. degrees from The University of Edinburgh, Edinburgh, U.K., in 2005 and 2009, respectively. He was a Visiting Student Research Collaborator with Princeton University, Princeton, USA, in 2008. From 2009 to 2012, he was a Postdoctoral Research Associate with the KTH-Royal Institute of Technology, Stockholm, Sweden. Since 2013, he has been with Tongji University, Shanghai, China, where he is currently an Associate Professor. He is currently taking a Marie Sklodowska-Curie Individual Fellowship at the University of Exeter, Exeter, UK. His research interests include information theory and signal processing for wireless communication networks, and data-driven research and applications for smart city and intelligent transportation systems.

PING WANG graduated from the Department of Computer Science and Engineering, Shanghai Jiao Tong University, and the Ph.D. degree, in 2007. He is currently an Associate Professor with the Department of Information and Communication Engineering, Tongji University. His main research interests include routing algorithms and resource allocation of wireless networks (especially for VANETs). He has also constructed the testing bed of cellular-based V2X in Shanghai.

YUSHENG JI (M'94–SM'18) received the B.E., M.E., and D.E. degrees in electrical engineering from the University of Tokyo. She joined the National Center for Science Information Systems (NACSIS), Japan, in 1990. She is currently a Professor with the National Institute of Informatics (NII) and The Graduate University for Advanced Studies (SOKENDAI), Japan. Her research interests include network architecture, resource management in wireless networks, and mobile computing. She is a TPC Member of the IEEE INFOCOM, ICC, GLOBECOM, and WCNC. She has served as a Board Member of Trustees of the IEICE, a Steering Committee Member of Quality Aware Internet SIG, and an Expert Member of the IEICE Technical Committees on Communication Quality. She has served as the Symposium Co-Chair of the IEEE GLOBECOM, in 2012 and 2014, and the Track Chair of the IEEE VTC 2016 Fall and 2017 Fall. She is also the Symposium Co-Chair of the IEEE ICC2020. She is an Expert Member of IEICE Technical Committees on Internet Architecture and a Steering Committee Member of Internet and Operation Technologies SIG of IPSJ. She has served as an Associate Editor of *IEICE Transactions* and IPSJ Journal. She is an Editor of the IEEE TRANSACTIONS OF VEHICULAR TECHNOLOGY.